Spring 2013

A friction prediction model for small SI engines

Avinash Singh

Department:

A FRICTION PREDICTION MODEL FOR SMALL SI ENGINES

by

AVINASH SINGH

A THESIS

Presented to the Faculty of the Graduate School of the

MISSOURI UNIVERSITY OF SCIENCE AND TECHNOLOGY

In Partial Fulfillment of the Requirements for the Degree

MASTER OF SCIENCE IN MECHANICAL ENGINEERING

2013

Approved by

James A. Drallmeier, Advisor
Kakkattukuzhy M. Isaac
Daniel S. Stutts

ABSTRACT

A substantial portion of the input fuel energy in an SI engine is lost towards overcoming the frictional forces from various rubbing parts. These frictional losses are very significant in small engines and these losses can be reduced by incorporating some design changes. A semi-empirical friction prediction model was studied and modified with the help of the experimental results for small SI engines. This model is dependent upon engine geometry and speed. The model divides the frictional work into different sub-assemblies of the engine and these sub-assemblies are in turn divided to determine the friction associated with individual components. A major advantage of this model is that it can predict frictional losses for a particular SI engine just by using its geometry and operating speeds. In addition, this model also accounts for the change in viscosity of the lubricant with respect to varying temperature. The new model will give the designers an overview of the distribution of frictional losses among the different components of the engine. Also, with the help of this information appropriate design changes can be made to reduce engine friction losses.

ACKNOWLEDGMENTS

Firstly, I would like to be grateful to my advisor Dr. James A Drallmeier for his guidance and immense support during the course of my graduate career. I am equally thankful to my committee members Dr. Daniel Stutts, Dr. Arindam Banerjee and Dr. Kakkattukuzhy M. Isaac for their patience and coaching towards my research.

I would also like to take this opportunity to thank Dr. Jeffery Massey, Shawn Wildhaber, Cory Huck, Joshua Bettis, Aaron Attebery and Allen Ernst. I am equally thankful to Joe Boze and Robert Hribar for their expertise in assembling the necessary equipment for the experimental setup.

Finally, I am forever grateful to my parents Hemprabha and Anil Kumar Singh for their unconditional support and guidance throughout my life. I am indebted to my grandparents and to all my friends for their tremendous support and care.

TABLE OF CONTENTS

Page

ABSTRACT..... iii

AKNOWLEDGEMENTS..... iv

LIST OF ILLUSTRATIONS x

LIST OF TABLES..... xiii

NOMENCLATURE..... xiv

SECTION

1. INTRODUCTION 1

2. BACKGROUND 3

2.1. FRICTION FUNDAMENTALS 3

2.1.1. Lubricated Friction..... 3

2.1.2. Turbulent Dissipation..... 5

2.2. ENGINE FRICTION..... 6

2.2.1. Components of Engine Friction. 6

2.2.2. Rubbing Friction 7

2.2.2.1 Crankshaft friction..... 8

2.2.2.2 Accessory friction..... 8

2.2.2.3 Valvetrain friction. 8

2.2.2.4 Reciprocating friction. 9

2.3. ENIGNE FRICTION DATA AND DEFINITIONS 13

2.3.1. Mean Effective Pressure. 13

2.3.2. Types of MEP 13
2.4. METHODS OF MEASURING ENGINE FRICTION 14
2.4.1. Measurement of FMEP from IMEP..... 14
2.4.2. Breakdown Motoring Test.. 15
2.4.3. Willians Line..... 16
2.4.4. Morse Test 16
2.5. LUBRICANTS..... 16
2.5.1. Function of Lubricants..... 16
2.5.2. Properties of Lubricants..... 17
3. APPROACH 18
4. EXPERIMENTAL SETUP AND TEST PROCEDURES 22
4.1. EXPERIMENTAL SETUP 22
4.2. SPECIFICATIONS OF TEST ENGINES 23
4.2.1. Engine 1 23
4.2.2. Engine 2 24
4.3. TEST PROCEDURES 25
4.3.1. Breakdown Motoring Test 25
4.3.2. Oil and Temperature Variation Test 27
4.4. DATA ANALYSIS 28
5. RESULTS FOR ENGINE 1..... 30
5.1. BREAKDOWN TEST RESULTS 30
5.2. OIL AND TEMPERATURE VARIATION TEST RESULTS 31
6. MODEL DESCRIPTION AND MODIFICATION 35

6.1. CRANKSHAFT FRICTION MODEL 36
6.1.1. Model Description 36
6.1.1.1 Bearing seal term. 36
6.1.1.2 Main bearing hydrodynamic friction term 37
6.1.1.3 Turbulent dissipation term 40
6.1.2. Results 40
6.2. ACCESSORY FRICTION MODEL 41
6.2.1. Model Description 41
6.2.2. Results 42
6.2.3. Modifications 42
6.3. VALVETRAIN FRICTION MODEL 45
6.3.1. Model Description 45
6.3.1.1 Camshaft bearing hydrodynamic friction term 45
6.3.1.2 Flat follower friction term 46
6.3.1.3 Oscillating hydrodynamic friction term 47
6.3.1.4 Oscillating mixed lubrication friction term 48
6.3.2. Results 49
6.3.3. Modifications. 49
6.4. RECIPROCATING FRICTION MODEL 51
6.4.1. Model Description 51
6.4.1.1 Reciprocating friction term 52
6.4.1.2 Piston ring friction term without gas pressure loading 53
6.4.1.3 Gas pressure loading term 54

6.4.1.4 Hydrodynamic journal bearing term 54

6.4.2. Results 54

6.4.3. Modifications. 55

6.5. INTRODUCTION OF VISCOSITY SCALING IN THE MODIFIED PNH MODEL 56

6.5.1. Concepts of Viscosity Scaling 56

6.5.2. Application of Viscosity Scaling to the Modified PNH Model 58

6.5.2.1 Crankshaft friction model 58

6.5.2.2 Accessory friction model 58

6.5.2.3 Valvetrain friction model 58

6.5.2.4 Reciprocating friction model 59

6.5.3. Comparison Between the Oil and Temperature Variation Test and Modified PNH Model Results 59

7. RESULTS FOR ENGINE 2 66

7.1. BREAKDOWN TEST RESULTS 66

7.2. PNH MODEL RESULTS 67

7.3. COMPARISION BETWEEN THE BREAKDOWN TEST AND MODIFIED MODEL RESULTS 68

8. SUMMARY 71

8.1. SUMMARY OF THE MODIFIED PNH MODEL 71

9. CONCLUSION 73

9.1. FRICTION PREDICTION PERFORMANCE OF THE MODIFIED PNH MODEL 73

9.2. MODEL LIMITATIONS 73

APPENDICES

A. INPUTS TO MODIFIED PNH MODEL 74

B. ADDITIONAL PLOTS…….. 76

BIBLIOGRAPHY 80

VITA 82

LIST OF ILLUSTRATIONS

Figure Page

2.1. Journal bearing 3

2.2. Stribeck curve 4

2.3. Energy distribution in an IC engine 6

2.4. Typical rubbing friction distribution in an engine 7

2.5. Valvetrain 9

2.6. Piston forces 10

2.7. Piston lubrication and pressure distribution in the lubricating oil film 11

2.8. Reynold's equation parameters 12

2.9. Depiction of pumping work through cylinder pressure-volume data 15

3.1. Approach used in this study 19

4.1. Experimental setup 22

4.2. Plates for the cylinder 25

4.3. Master weights 26

4.4. Cartridge heater in the crankcase 28

4.5. An example of a data analysis plot 29

5.1. Motoring FMEP at different speeds 30

5.2. Motoring FMEP at different speeds and temperatures for SAE 5W20 31

5.3. Motoring FMEP at different speeds and temperatures for SAE 10W30 32

5.4. Motoring FMEP at different speeds and temperatures for SAE 10W40 32

5.5. Motoring FMEP at different speeds and temperatures for SAE 30 33

5.6. Motoring FMEP at different speeds and temperatures for SAE 40 33

5.7. Motoring FMEP at different speeds and temperatures for SAE 50 34

6.1. Model FMEP at different speeds 35

6.2. Bearing seal 36

6.3. Sleeve bearing 37

6.4. Rotating cylinder viscometer 38

6.5. Experimental vs. model friction for the crankshaft 41

6.6. Experimental vs. model friction for crankshaft and oil pump 42

6.7. Experimental vs. modified model friction for crankshaft and oil pump 44

6.8. Flat follower assembly 46

6.9. Experimental vs. model friction for crankshaft, oil pump and valvetrain 49

6.10. Experimental vs. modified model friction for crankshaft, oil pump and valvetrain 51

6.11. Piston assembly 52

6.12. Experimental vs. model friction for crankshaft, oil pump, valvetrain and piston group 55

6.13. Experimental vs. modified model friction for crankshaft, oil pump, valvetrain and piston group 56

6.14. Model vs. experimental results for temperature variation at 1500 rpm 60

6.15. Model vs. experimental results for temperature variation at 2000 rpm 60

6.16. Model vs. experimental results for temperature variation at 2500 rpm 61

6.17. Model vs. experimental results for temperature variation at 3000 rpm 61

6.18. Model vs. experimental results for temperature variation at 3400 rpm 62

6.19. Model vs. experimental results for oil SAE 5W20 at 3000rpm 62

6.20. Model vs. experimental results for oil SAE 10W40 at 3000rpm 63

6.21. Model vs. experimental results for oil SAE 30 at 3000rpm 64

6.22. Model vs. experimental results for oil SAE 40 at 3000rpm 64

6.23. Model vs. experimental results for oil SAE 50 at 3000rpm 65

7.1. Motoring FMEP at different speeds..... 66

7.2. Model FMEP at different speeds 67

7.3. Experimental vs. modified model friction for crankshaft assembly 68

7.4. Experimental vs. modified model friction for crankshaft, oil pump..... 69

7.5. Experimental vs. modified model friction for crankshaft, oil pump and valvetrain. 69

7.6. Experimental vs. modified model friction for crankshaft, oil pump, valvetrain and piston group 70

8.1. Variation of FMEP with temperature and engine speed..... 71

LIST OF TABLES

Table Page

4.1: Engine 1 Specifications 23

4.2: Engine 2 Specifications 24

NOMENCLATURE

Symbol	Description
D_b	Bearing Diameter
B	Bore
S	Stroke
n_c	Number of Cylinders
L_b	Length of the bearing
n_b	Number of bearings
N	Speed
S_p	Mean piston speed
P_i	Intake pressure
P_a	Atmospheric pressure
r_c	Compression ratio
n_v	Number of valves
L_v	Maximum Valve lift
V	Velocity
$\dot{m}$	Mass flow rate
r_e	Exhaust valve diameter
MEP	Mean Effective Pressure (kPa)
T	Torque (Nm)
n_r	Number of revolution per cycle
$\forall_d$	Displacement Volume

K	Friction reduction coefficient (Acquired from experiment; not to be confused with coefficient of friction)
σ	Loading force per unit area
μ	Viscosity of the fluid (lubricant)
c	Bearing clearance
N	Speed
B	Bore
D_b	Bearing diameter
L_b	Bearing length
n_b	Number of bearings
n_c	Number of cylinders
U	Sliding speed
$\frac{\partial h}{\partial t}$	Extension speed of oil film thickness
V	Velocity
L_s	Skirt length
F_n	Normal force
$FMEP$	Frictional mean effective pressure
p_i	Intake Pressure
p_a	Atmospheric pressure
K	Constant
$\dot{W}_{shaft}$	Power
S_p	Mean piston speed
$CMEP$	Crankshaft mean effective pressure

AMEP	Accessory mean effective pressure
VMEP	Valvetrain mean effective pressure
RMEP	Reciprocating mean effective pressure
BST	Bearing seal term
MBHT	Main bearing hydrodynamic term
TDT	Turbulent dissipation term
FFT	Flat follower term
OHLT	Oscillating hydrodynamic lubrication term
OMLT	Oscillating mixed lubrication term
PST	Piston skirt term
PRFT	Piston ring friction term
HJBT	Hydrodynamic journal bearing term
GPLT	Gas pressure loading term

1. INTRODUCTION

The fuel efficiency of an internal combustion engine is affected by various factors, one of them is rubbing friction. Rubbing friction in an engine is the result of the interaction between two moving surfaces. The early study of engine friction started in late 1950s (1). Different test procedures and prediction models were developed to determine engine friction. These studies were mainly directed towards large automotive engines. A strong focus was never given to study the rubbing friction in small air cooled SI (Spark Ignited) engines. Small air cooled SI engines are mainly used in farm equipment and industrial applications. In an effort to understand and improve the fuel efficiency of small SI engines, the rubbing frictional losses present in small engines were investigated in this study.

The aim of this study was to develop a rubbing friction prediction model for small air cooled SI engines. As compared to the large automotive engines, the small engines have a relatively simple design, for example, they use sleeve bearings in place of ball bearings. The sleeve is machined in the part itself. This is done to keep the cost of the engine low. Therefore, the prediction models, developed in the past for automotive engines, were not able to accurately capture the trends in the small engine friction. This investigation spans the study of different components of rubbing friction, engine friction test procedures and prediction models, to modify a pre-existing friction prediction model (the PNH model) (2) to account for the frictional behavior of small industrial engines.

During the course of this study, different factors affecting the engine rubbing friction were studied, in detail, along with the test to determine the friction contribution from the individual components of the engine. The data from the test was used to modify

a pre-existing friction prediction model for accurate prediction results. The modified model was then applied to a different engine to validate the accuracy of the friction prediction model.

2. BACKGROUND

In an engine, the work generated at the piston is more than the useful work available at the crankshaft. This loss in work between the engine cylinder and crankshaft occurs usually due to friction. Friction is the resisting force which opposes the relative motion between two solid surfaces, fluid layers or fluids trapped in between two solid surfaces. The work associated with friction is called friction work. The energy released through the combustion of the fuel inside the engine cylinder is the Indicated work. Friction work consumes a large portion of the Indicated work, varying between 10% at full load to 100% at no-load (3).

2.1. FRICTION FUNDAMENTALS

2.1.1. Lubricated Friction. Different friction states occur due to the types of lubrication regimes prevailing at different locations in an engine. Figure 2.1 shows an example of the lubricated friction in a journal bearing. The arrows in the oil film indicate the turbulent agitation of the lubricating oil.

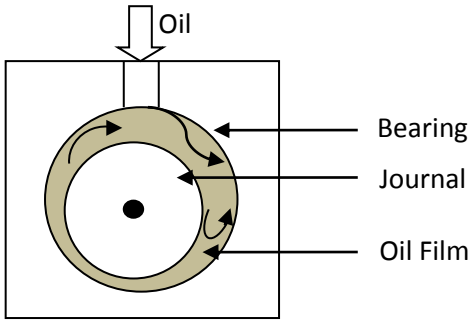

Figure 2.1. Journal bearing

Different lubrication regimes can be explained by the Stribeck curve. The Stribeck curve in Figure 2.2 gives a description of the different types of lubrication regimes present between two surfaces. The Stribeck curve is a plot of the coefficient of friction with respect to the non-dimensional duty parameter $\mu N/\sigma$, where μ the dynamic viscosity of the lubricant, N is the rotational speed of the shaft and σ is the loading force per unit area.

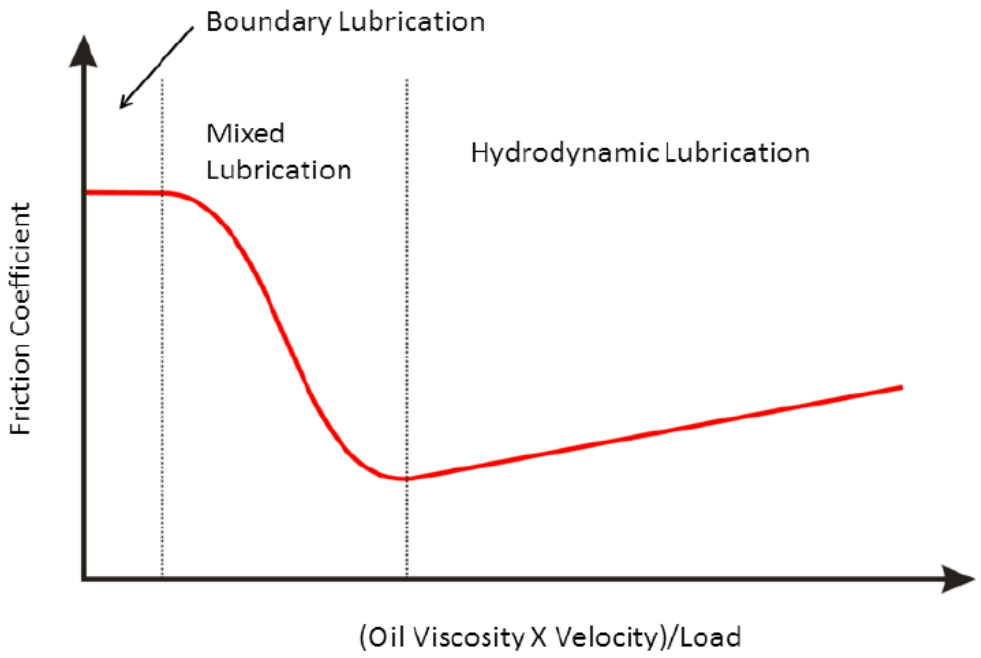

Figure 2.2. Stribeck curve

According to the Stribeck curve there are mainly three types of lubrication regimes. Boundary lubrication is the type of lubrication in which the two rubbing surfaces are in direct contact with each other. In Hydrodynamic lubrication there is a distinct separation between the two rubbing surfaces, this separation is caused by the lubricant. Since there is a distinct separation between the journal and the bearing surface due to the oil film in Figure 2.1, this type of lubrication falls under the hydrodynamic regime. Lastly, the mixed lubrication is the combination of both hydrodynamic and boundary lubrication. This means there is a partial contact between the two rubbing surfaces. It can be clearly seen from Figure 2.2 that the friction coefficient is the highest for the boundary lubrication, it reduces drastically in the mixed lubrication region. The coefficient of friction is the lowest in the hydrodynamic region. As the speed increases the friction coefficient linearly increases. This is due to the increased velocity gradient with increased across the lubricant with increase in rotational speed. All three types of lubrication regimes are present across the different assemblies of an internal combustion engine. For example, a piston assembly has both boundary and hydrodynamic lubrication due to the oscillating motion.

2.1.2. Turbulent Dissipation. Turbulent dissipation is the work required to pump or circulate fluids across the engine. As different fluids such as lubricating oil, cooling water or air is circulated through the engine, the work done to initiate the flow of these fluids is dissipated through turbulence. The frictional forces involved in turbulent dissipation are proportional to the square of engine speed. Turbulent dissipation is present in the bearings. It is mainly the work required to circulate the lubricating oil through the restriction of the bearings.

2.2. ENGINE FRICTION

2.2.1. Components of Engine Friction. The useful power at the output of an internal combustion engine is lower than the power produced at the piston. This difference between the powers is due to friction. This frictional loss is a collective contribution from different components present in an engine for example, piston assembly, crankshaft bearing etc. Figure 2.3 shows the distribution of the input fuel energy in an engine.

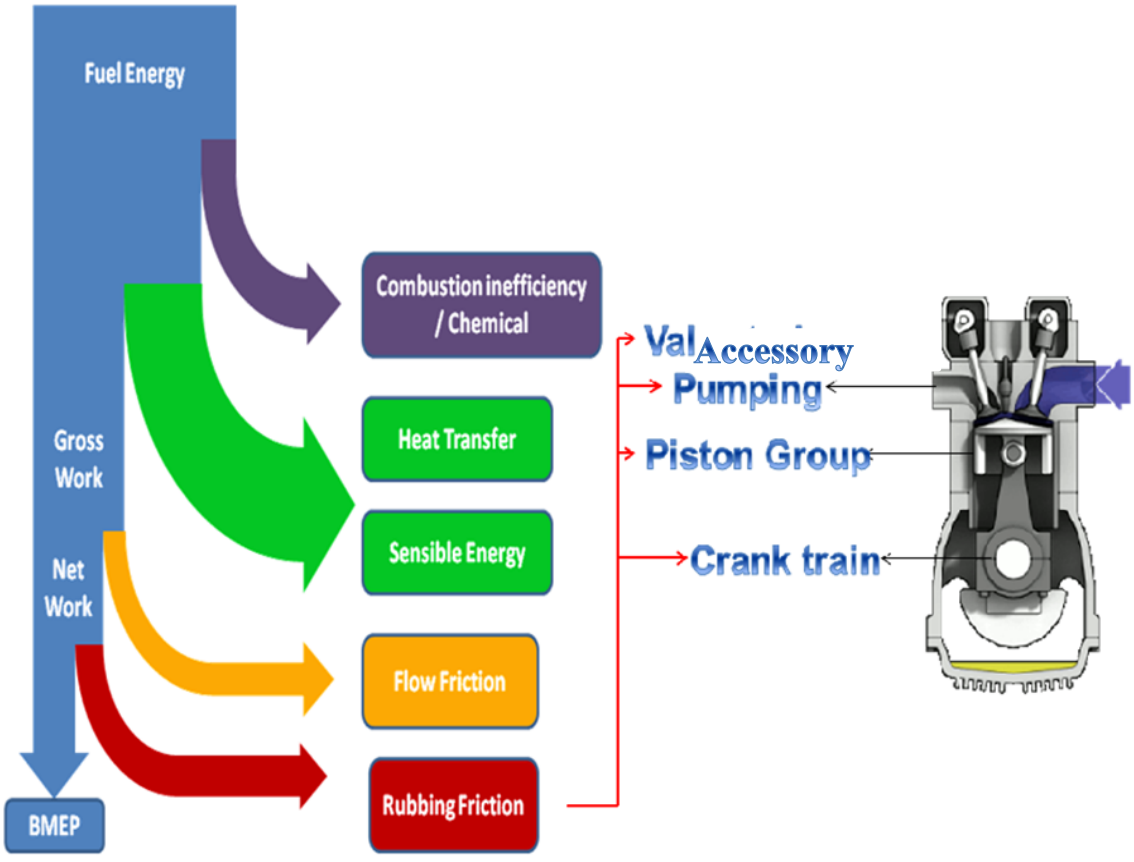

Figure 2.3. Energy distribution in an IC engine

Engine friction if mainly divided into four parts as shown in the figure. Apart from the rubbing friction, pumping friction is also part of the lost work produced by the engine, it is also known as the Flow friction. Pumping friction is a combination of throttling and valve flow work and is beyond the scope of this investigation. A detailed description of the rubbing friction is given below.

2.2.2. Rubbing Friction. The total engine rubbing friction is the combination of friction from all the sub-assemblies and accessories of the engine. Different assemblies of the engine which contribute to the total frictional losses are shown in Figure 2.4, they are:

1. Crankshaft friction
2. Accessory friction
3. Valve Train friction
4. Piston Assembly friction

Generally the trends show, that piston assembly contributes approximately 50% of the total and accessory rubbing friction (4).

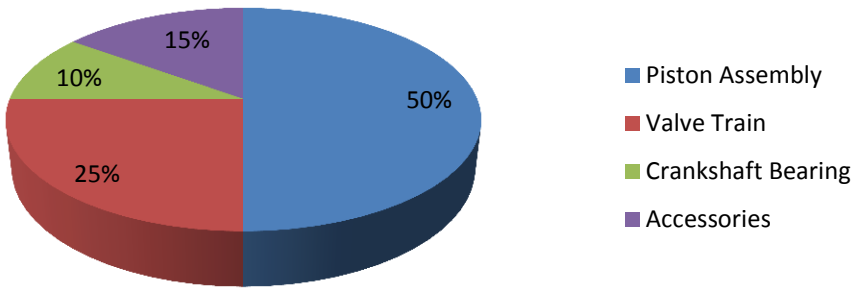

Figure 2.4. Typical rubbing friction distribution in an engine

Friction related to engines has been investigated through different methods. A particular emphasis has been placed on the study of friction related to the piston assembly (5). Before getting into the detailed description of the frictional parameters a brief introduction to different lubrication regimes present in the sub-assemblies of the engine is important to understand the type of frictional interaction between the different parts of an engine.

2.2.2.1 Crankshaft friction. The friction contribution of the crankshaft is mainly due to the bearings and the bearing seals. Bearings operate in the hydrodynamic range, some amount turbulent dissipation is also present due to the flow of the lubricant through the bearing restrictions. The frictional force can be calculated by the product of bearing area and the mean velocity gradient. This particular term is derived from a simple problem of fluid between two rotating cylinders (Section 6.1.1.2). A linear velocity profile for the fluid was considered in this case.

2.2.2.2 Accessory friction. Accessory losses are the losses associated with built-in parts like the oil pump, fuel pump etc. These losses contribute up to 20% of the total frictional losses. These losses are generally assumed to a function of speed (Section 6.2).

2.2.2.3 Valvetrain friction. A valve train mainly consists of camshaft, follower, rocker arm, spring, retainer etc. A depiction of a valve train is described in the Figure 2.5. There are two main forces which provide frictional loading during the operation of a valve train. The first is the spring force, this force is significant only at low speeds. The second is the inertial force. The inertial forces become more significant at high speeds (2). Different approaches for reducing the valvetrain friction are: reduced loading of the spring and reduction in mass of the valve, usage of tappet roller cam followers and use of

needle bearings for rocker arm. Roller cam followers greatly reduce the valve train friction (6); they can be used to reduce the friction to almost half its original value.

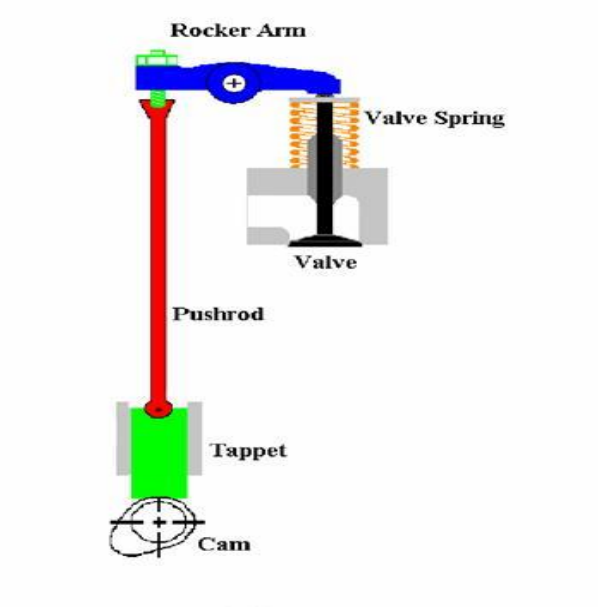

Figure 2.5. Valvetrain

2.2.2.4 Reciprocating friction. A number of different forces act on the piston during the reciprocating motion. The free body diagram given in Figure 2.6 shows the forces acting on the piston. Piston forces mainly consists of the gas force which acts on the top surface of the piston. The gas force is the result of the compressed air/fuel mixture and the products of combustion inside the engine cylinder. The inertial force is present due to the mass of the piston. In addition to these forces, a frictional force due to the interaction between the piston rings and the cylinder wall along with the side force due to the connecting rod are also present. The piston skirt carries the side load caused by the

angular orientation of the connecting rod with respect to the cylinder axis. The piston rings contribute a substantial amount towards the engine friction.

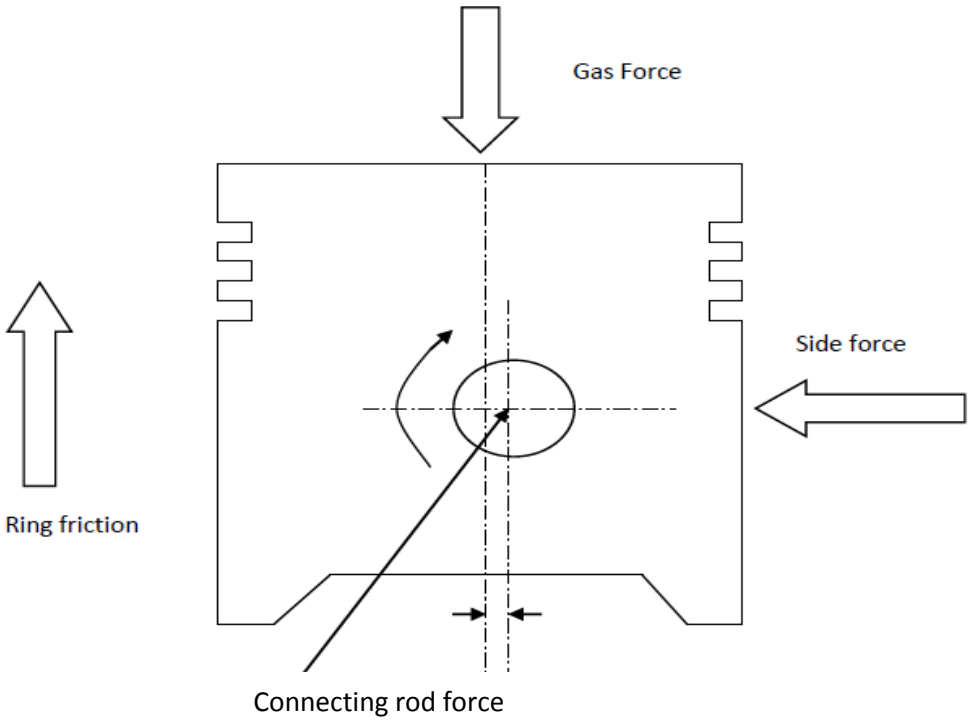

Figure 2.6. Piston forces

There are mainly two types of piston rings: compression and oil control rings. The main functions of piston rings are as follows:

1. Provide proper seal and gas pressure for the cylinder gases
2. Provide necessary lubrication to the cylinder wall and piston interface to reduce friction
3. Transfer heat from the piston to the cylinder walls

The top ring is the compression ring. It has an axial profile i.e. curved outer edge to facilitate hydrodynamic lubrication. The subsequent compression rings reduce the pressure drop across the first ring. As mentioned earlier, the piston assembly is the major contributor for the total engine friction. The forces responsible for friction due to piston rings are shown in the Figure 2.7.

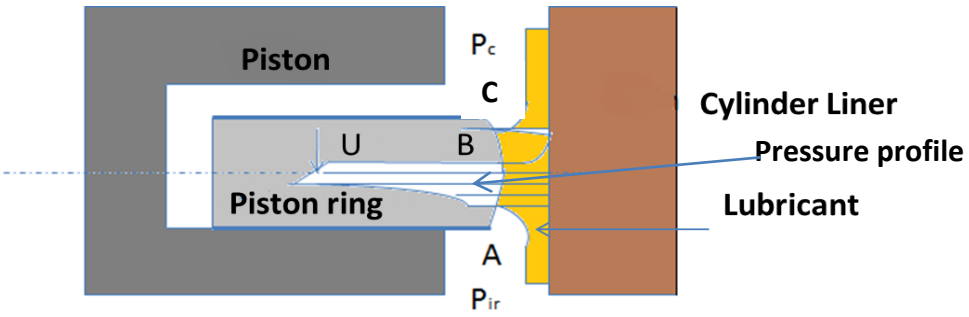

Figure 2.7. Piston lubrication and pressure distribution in the lubricating oil film

In Figure 2.7, P_c is the cylinder pressure and P_{ir} is the pressure between the first and second rings (Inter-ring gas pressure). P_c acts on the top part of the ring and P_{ir} acts on the oil film and the bottom part of the ring. Due to the frequent change in the direction of motion of the piston, the ring keeps shifting between the top and the bottom surface of the piston groove. The pressure on the oil film is generated as depicted by surfaces A and B during the downward motion of the ring. C-B is the pressure generating surface in the reverse direction. The equation which models the behavior of the oil film between two surfaces is called Reynold's equation (3). This equation is derived from Navier-Stokes equation for liquid film motion. The equation is as follows:

$$\frac{\partial}{\partial x}\left(\frac{h^3}{\mu}\frac{\partial p}{\partial x}\right)=6U\frac{\partial h}{\partial x}+12\frac{\partial h}{\partial t} \quad (1)$$

Here *h* is the thickness of the film, *x* the width of the film, *U* is the relative velocity between the rubbing surfaces and μ is the viscosity of the lubricant. Figure 2.8 shows the parameters of the Reynolds's equation.

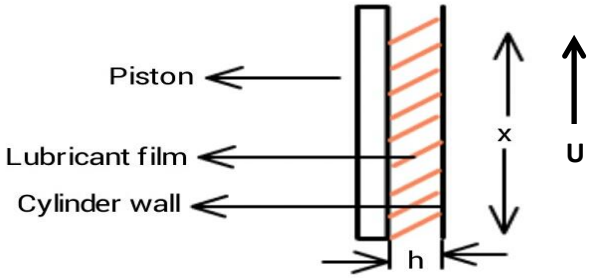

Figure 2.8. Reynold's equation parameters

It has been observed (2) that the thickness of the lubricant film between the cylinder and the piston is the lowest at Top Dead Center (TDC). The oil film thickness increases with decreasing load and increasing velocity. Higher lubricant temperatures cause a decrease in film thickness due to the reduced viscosity of the lubricating oil. Apart from the rings, the piston skirt is also a contributor to engine friction. The piston skirt facilitates hydrodynamic lubrication due to larger surface area. Two types of lubrication regimes exist in piston-liner interaction. Firstly, the hydrodynamic lubrication

is significant during increasing speeds. The piston skirt-liner usually operates in the hydrodynamic regime. Secondly, the boundary lubrication becomes relevant with increasing load in the piston ring and liner interaction.

These components together form the total friction losses of the engine. These losses are undesirable. Researchers have revisited this problem in the past to reduces the frictional losses and improve the efficiency of the engines. An overview of the previous approaches to determine frictional losses will be described in the Section 2.4.

2.3. ENIGNE FRICTION DATA AND DEFINITIONS

2.3.1. Mean Effective Pressure. Mean Effective pressure (MEP) refers to the work done per cycle per unit displaced volume. It is a convenient way of observing the work distribution to each process.

$$\mathrm{MEP}=\frac{W_c}{V_d} \tag{2}$$

2.3.2. Types of MEP. $IMEP_g$ - Gross indicated mean effective pressure is the work delivered to the piston over compression and expansion per cycle per unit displaced volume.

$IMEP_n$ - Net indicated mean effective pressure is the work delivered to the piston over all 4 strokes of a cycle per unit displaced volume.

RFMEP - Rubbing frictional mean effective pressure. It represents losses due to motion between parts (rubbing) in the engine.

AMEP - Accessory mean effective pressure.

BMEP - Brake mean effective pressure, determined from the measured engine torque.

2.4. METHODS OF MEASURING ENGINE FRICTION

Engine friction can be determined by subtracting the brake power output from the indicated power. The indicated power can be obtained by collecting accurate in-cylinder pressure data. This technique is not very effective with a multi cylinder engine due to cylinder to cylinder variability in the indicated power. Also, accurate collection of pressure data involves high cost. Therefore, frictional losses in an engine are usually determined by motoring tests. A few common techniques to determine engine friction have been described below.

2.4.1. Measurement of FMEP from IMEP. Gross indicated mean effective pressure (IMEP) is calculated by integrating the cylinder pressure-volume data over the compression and expansion strokes. Accurate measurement of the pressure data is required for good results. Both gross indicated mean effective pressure and pumping mean effective pressure (PMEP) can be obtained using this technique. The mean effective pressure (MEP) can be calculated using the pressure data from the fired (running the engine) engine. The PMEP (Pumping Mean Effective Pressure) is the value of the area inside the curve of the pumping loop. The conventional definition of pumping work is depicted in Figure 2.9; it is the sum of the shaded area A and the shaded area B divided by the displacement volume of the engine. The trapezoidal rule is used to integrate the pressure data over the required duration.

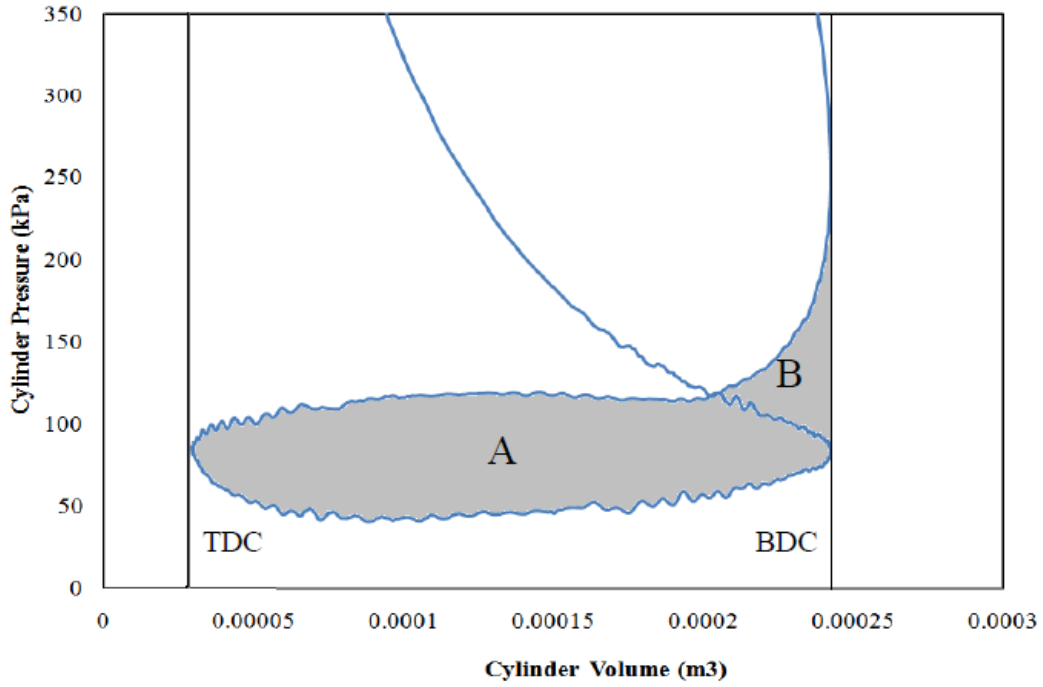

Figure 2.9. Depiction of pumping work through cylinder pressure-volume data

The following equations are used to acquire the total frictional mean effective pressure, TFMEP.

$$IMEP_g = IMEP_n + PMEP \quad (3)$$

$$TFMEP = PMEP + RFMEP + AMEP \quad (4)$$

$$BMEP = IMEP_g - TFMEP \quad (5)$$

$$BMEP = IMEP_n - RFMEP - AMEP \quad (6)$$

2.4.2. Breakdown Motoring Test. Direct motoring tests are used to determine the contribution of friction losses from different sub-assemblies. If the engine is run

closely to the operating conditions i.e. the fired condition. At the fired conditions, the engine is at a relatively higher oil temperature and pressure than the motoring conditions, therefore, during a motoring test the oil temperature and pressure should be maintained close to actual firing conditions for realistic results. The breakdown motoring test is a good indicator for the individual contribution of different parts to frictional losses. This approach will be used extensively in this study and a detailed description of this approach has been provided in Section 4.3.1.

2.4.3. Willians Line. This method is mainly used for diesel engines. A plot of fuel consumption and brake power output is obtained and extrapolated to zero fuel consumption. The drawback of this test is the difficulty involved in accurately extrapolating the curve.

2.4.4. Morse Test. This test involves cutting out (i.e. to stop combustion) of individual cylinders in a multi cylinder engine. The engine is maintained at the same speed with the help of other cylinders. Since the other cylinders drive the cut out cylinder, the reduction in brake torque is the friction associated with the cut out cylinder. Care must be taken that the cutting out of an individual cylinder does not significantly affect fuel flow to the remaining cylinders.

2.5. LUBRICANTS

2.5.1. Function of Lubricants. A lubricant mainly performs four essential functions inside an engine. These functions are listed below.

1. Reduce friction between the rubbing surfaces of the engine.
2. Dissipate the heat to the external walls to avoid overheating of the engine.
3. Provide a good seal between the engine cylinder and the crankcase.

4. Constantly clean the impurities and residues from the lubricated components.

2.5.2. Properties of Lubricants. There are three desired properties for a lubricant which makes it suitable for use in engine application. Firstly, the oxidation stability; as the engine is subjected to high temperature and pressures, it is important that the lubricant stays chemically stable throughout the entire range of pressure and temperature. Secondly, the detergency, it the capability of the lubricant to remove the residues and deposits formed as the results of combustion. Thirdly, the viscosity, a lubricant should have just the right viscosity to facilitate cold starts and also provides adequate sealing when the engine is fully warmed up. The actual viscosity grade of a lubricant is determined by the Society of Automotive Engineers, for example SAE 15W40 for multigrade oil and SAE 40 for a monograde oil. The 15W refers to the viscosity grade at low temperatures (W from winter), whereas the second number 40 refers to the viscosity grade at high temperature.

The background defined in this section was used to build an appropriate approach for developing and validating a friction prediction model for small SI engines. A description of the approach planned for this study is given in the next section.

3. APPROACH

Figure 3.1 describes the approach followed during the course of this study. The total engine rubbing friction is the sum of crankshaft, auxiliary, valvetrain and piston assembly friction. These friction components were expressed in terms of their respective Mean Effective Pressure (MEP).

A pre-existing model called the PNH model (2) was used as a basis for developing a friction prediction model for small SI engines. The PNH model is abbreviated after the authors of the model: Patton, Nistchke and Heywood. The PNH model was initially designed for large automotive engines. The PNH model (2) for rubbing and auxiliary losses was based on the operating and design parameters of the engine. The pumping losses were calculated through the pressure drop across the intake and exhaust system. The general approach used by the PNH model for modeling the rubbing friction contribution from different sub-assemblies of the engine is as follows. Firstly, the coefficient of friction was related to the above mentioned dimensionless duty parameter, $\mu N/\sigma$ (Section 2.1.1), which is the function of viscosity, velocity and unit load. An assumption of the type of lubrication regime is required to develop the model. Secondly, the friction coefficient was multiplied with the normal force to obtain the frictional force. This frictional force was multiplied by the velocity to generate the power term. This power term was divided by the engine speed and the displacement volume to get Frictional Mean Effective Pressure (FMEP). The two factors namely velocity and normal force are a function of the interface geometry. The derived terms were calibrated with the constants acquired from the curve fit on the experimental results from the motoring tests. Least square regression was used to obtain the constants.

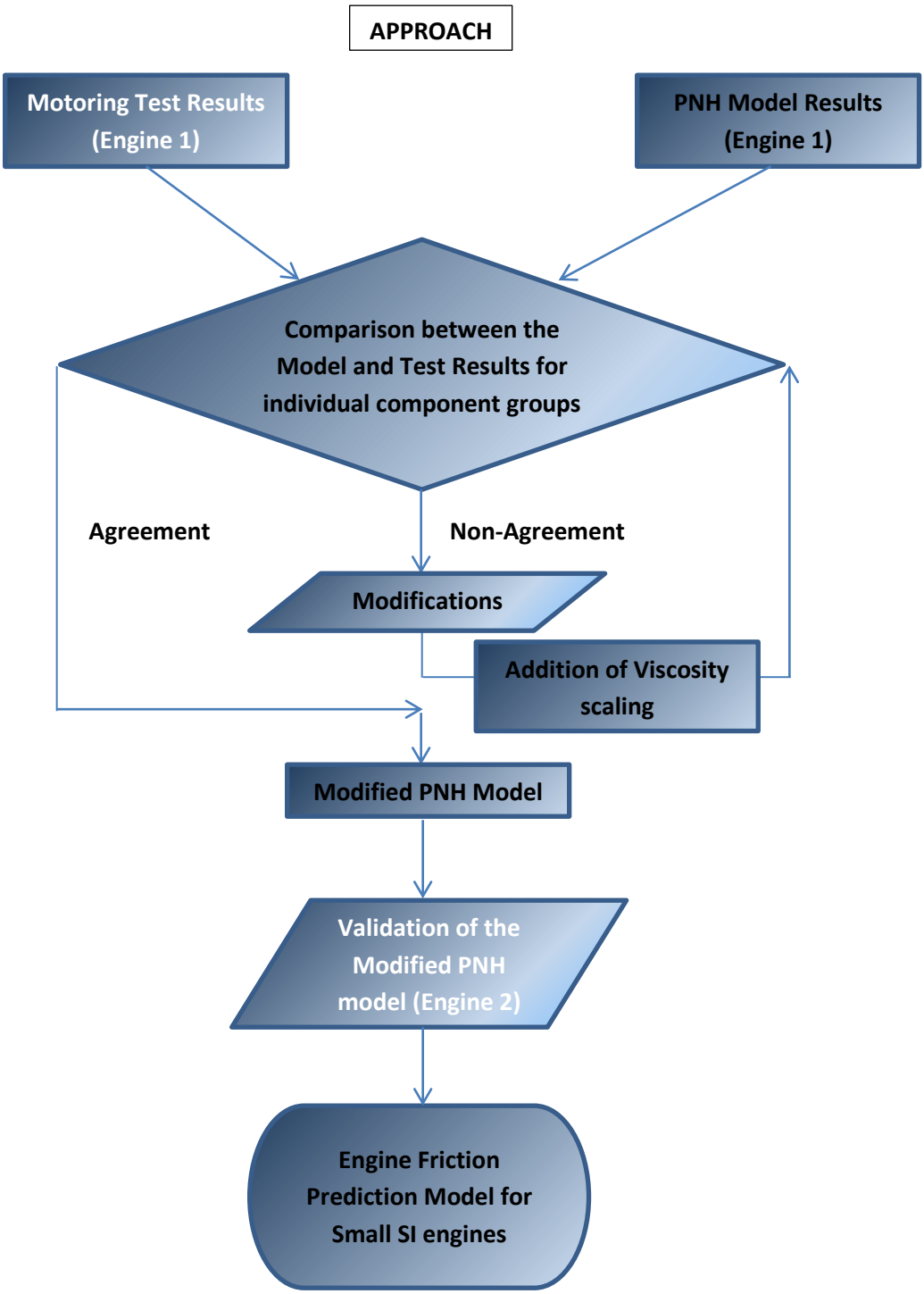

Figure 3.1. Approach used in this study

The following models were developed for the major contributors to the total engine:

1. Crankshaft friction model
2. Reciprocating friction model
3. Valve train friction model
4. Auxiliary friction model

The PNH model is mainly affected by the design dimensions and the speed of the engine. The model incorporates changes in design, for instance; the calibration coefficients for a V-engine are different from that of an inline engine. A detailed description of the PNH model has been provided in Section 6.

There were two small SI engines used in this study, Engine 1 and Engine 2 (The specification of the two engines is been described in Section 4.2). Firstly, Engine 1 was subjected to a motoring breakdown test. Simultaneously, the PNH model was applied to the test Engine 1. Secondly, the results from both the motoring test and the PNH model were compared for individual component groups of the engine (crankshaft assembly friction, auxiliary friction, valvetrain friction and piston assembly friction). Thirdly, the model components which were not in agreement with the motoring breakdown test were modified. After the modification the results from the modified model were compared again to the results from the motoring breakdown test. This process was repeated until all the individual component groups matched with the experimental results. After all the modifications, the modified PNH model was validated against Engine 2. Lastly, the individual modified sub model for each component group was assembled to form the complete friction prediction model.

A viscosity scaling was also applied to the PNH model in addition to the other modifications. Engine 1 was subjected to an oil and temperature variation test. The detail of this test is been defined in Section 4.3.2. The viscosity scaling helped the model to be flexible across the range of temperatures and oils.

4. EXPERIMENTAL SETUP AND TEST PROCEDURES

4.1. EXPERIMENTAL SETUP

The engine friction test stand in Figure 4.1 consisted of a vertically mounted dynamometer fixed to the stand along with the belt drive system. The dynamometer was coupled with a reaction torque transducer (Lebow model 2404-5k). This torque transducer measured the amount of torque required to motor the engine. The block diagram below gives a representation of the setup. The signal output from the torque transducer was collected through DAQ (Data Acquisition) readout (Daytronics 3578).

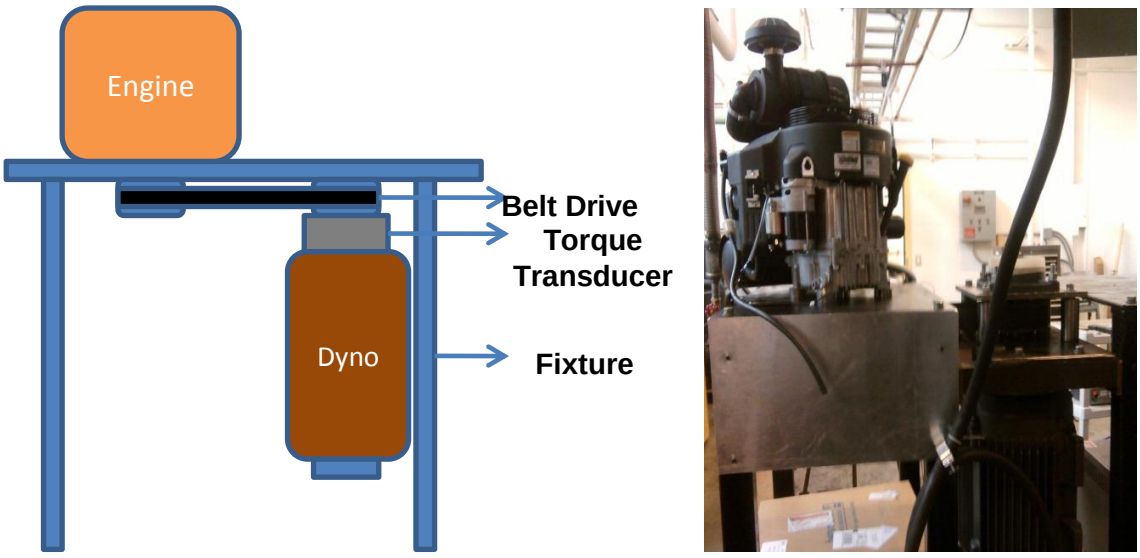

Figure 4.1. Experimental setup

Apart from the torque data, other parameters were collected using an oil pressure gauge and a type K thermocouple. Also, to control the oil temperature a type K cartridge

heater (Omega RINO 130/120V, Maximum Temperature: 100^{o}C) was used along with a controller (Omega CN7833). The engine was subjected to a breakdown test using the above given setup. The steps of the motoring breakdown test procedure have been described in detail later in this section.

4.2. SPECIFICATIONS OF TEST ENGINES

4.2.1. Engine 1. The friction prediction (PNH) model was modified and calibrated with respect to this particular engine. Engine 1 was subjected to a complete breakdown test. In addition to the breakdown test Engine 1 was also motored with different grades of oils. The specifications of this engine are listed in Table 4.1.

Table 4.1: Engine 1 specifications

Engine Type	Forced Air-Cooled, V-twin, 4-cycle, Vertical Shaft, OHV, Gasoline Engine
Number of Cylinders	2
Bore x Stroke	3.33 x 2.99 in. (84.5 x 76mm)
Displacement	852cm^3 (52 cu. in.)
Compression Ratio	8.2:1
Maximum Power	27.0hp (20.1 kW)/ 3600 rpm
Maximum Torque	44.6 ft. lbs. (60.5 N•m)/ 2400 rpm
Oil Capacity	2.1 U.S. qt. (2.0 liter) w/Filter
Dry Weight (without muffler)	124.0 lbs. (56.4kg)

4.2.2. Engine 2. The fundamental design of Engine 2 is similar to Engine 1. The major design differences are the number of valves, bearing sizes and the displacement volume. A breakdown test was also conducted on the Engine 2. This was done to evaluate the modified friction prediction model against a slight change in the design of the engine. The specifications of this engine are listed in Table 4.2.

Table 4.2: Engine 2 specifications

Engine Type	Forced Air-Cooled, V-twin, 4-cycle, Vertical Shaft, OHV, Gasoline Engine
Number of Cylinders	2
Bore x Stroke	3.5 x 3.15 in. (89.15 x 80mm)
Displacement	999cm^3 (61 cu. in.)
Compression Ratio	8.4:1
Maximum Power	35.0hp (26.1 kW)/ 3600 rpm
Maximum Torque	56.0 ft. lbs (75.9 N•m)/ 2800 rpm
Oil Capacity	2.0 U.S. qt. (1.9 liter) w/Filter
Dry Weight (without muffler)	138.0 lbs. (62.6kg)

4.3. TEST PROCEDURES

4.3.1. Breakdown Motoring Test. A breakdown or strip motoring test (7) is used to determine FMEP contribution from individual components of the engine. The FMEP was calculated from the measured motoring torque, engine speed and the displacement volume ($2\pi n_r T/V_d$)(Equation 2).

a) Before the actual breakdown measurements, the complete engine is motored at a particular speed and the oil pressure and temperature is maintained close to the firing conditions. This gives the total torque for both the mechanical friction and pumping losses (These are the flow losses across the intake and exhaust systems). Along with the torque, the oil pressure, temperature and the oil volumetric flow rate for the engine are also recorded, to maintain the operating conditions consistent through the complete breakdown procedure.

b) The cylinder heads are removed and replaced by plates to maintain strain conditions of the engine block. The head plates are shown in Figure 4.2.

Figure 4.2. Plates for the cylinder

The strain caused due to the tightening of the cylinder head bolts affects the tension on the piston rings, thereby affecting friction. When the cylinder is open the piston is not subjected to gas pressure forces. The oil pressure is maintained at the measured value to determine the engine friction without the pumping losses.

c) Next, the pistons and the connecting rods are removed to determine the crankshaft bearing friction. The rotating mass imbalance due to the absence of the piston and connecting rods in the crankshaft is compensated by using “master weights” (master weights are counter weights calculated through a dynamic mass balance of crankshaft piston assembly which are used to balance the rotating crankshaft). These master weights (Figure 4.3) were designed to clamp on to the crankshaft at the connecting rod slot with a clearance from the crankcase walls. The oil pressure and temperature is maintained in a similar manner as that of the previous step.

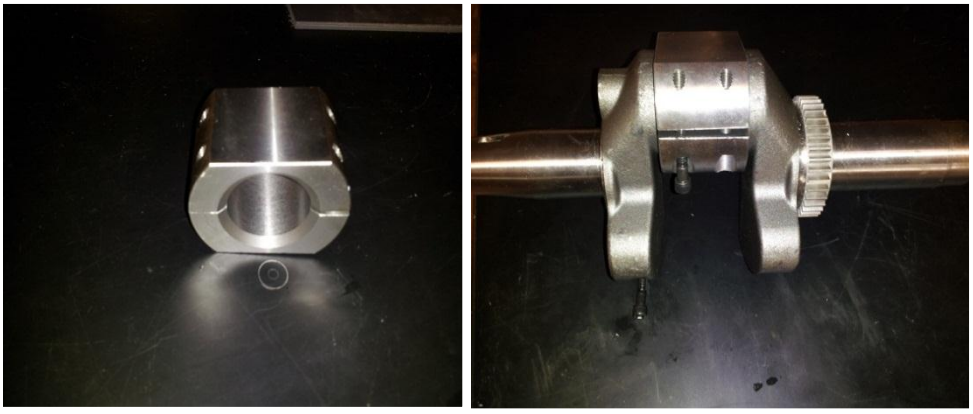

Figure 4.3. Master weights

d) Subsequently the test engine is motored in the absence of the valvetrain and the FMEP was recorded at specified oil pressure and temperatures. This step determines the friction due to the crankshaft (with master weights) and the oil pump. Measurement of the friction loss of the crankshaft along with the oil pump (if available) is completed at the specified oil pressures. The engines used in this study were equipped with an oil pump which was inbuilt inside the crankcase.

f) Lastly, the frictional losses for the crankshaft without the other accessories like the oil pump, coolant pump, alternator etc. is measured. None of the other accessories except the oil pump were present in the test engines for this study.

The test data points were recorded at 1500, 2000, 2500, 3000 and 3400rpm. The test data points were evenly distributed across the complete speed range of the test engines. The sum of all the individual frictional losses of different components gives the total friction of the engine. This is purely mechanical friction loss, it does not include the pumping losses.

4.3.2. Oil and Temperature Variation Test. In this test, the motoring torque of Engine 1 was recorded at different oil temperatures between 40 ^{o}C to 100 ^{o}C, in the steps of 10 ^{o}C. Engine 1 was also subjected to multiple grades of oils. Six different grades of lubricating oils namely, SAE 5W20, SAE 10W30, SAE 10W40, SAE 30, SAE 40 and SAE 50 were used in the oil variation test. The temperature control was achieved using cartridge heater and a controller. A 0.75 inch hole was made in the crankcase of Engine 1 to accommodate the cartridge heater (Figure 4.4). The reasoning behind the oil and temperature variation test was to determine the variation in the motoring torque with the

change in viscosity of the oil. The same data set point defined in Section 4.3.1 were used. The engines were completely drained and cleaned between different oil changes.

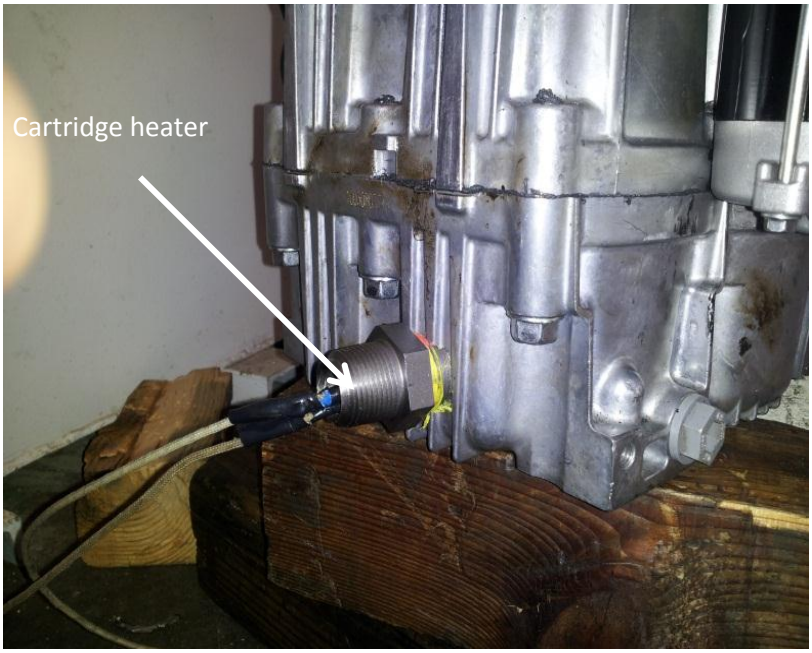

Figure 4.4. Cartridge heater in the crankcase

4.4. DATA ANALYSIS

The engine friction is measured by the amount of torque required to motor the engine at a particular speed. This torque is further converted to FMEP using Equation 2. As the engine friction is highly dependent on speed, the FMEP is always analyzed in conjunction with the engine speed. Each test point was repeated 5 times in random order to check for the repeatability of results. The uncertainty of the torque transducer was also plotted to check the integrity of the experimental torque values. Figure 4.5 shows a typical plot of experimental versus model FMEP for the crankshaft assembly at different

speeds. The error bars at each speed set point denotes the uncertainty from the torque transducer only. The line in red indicates the predicted model FMEP values and the line in blue shows the experimental results at different speeds.

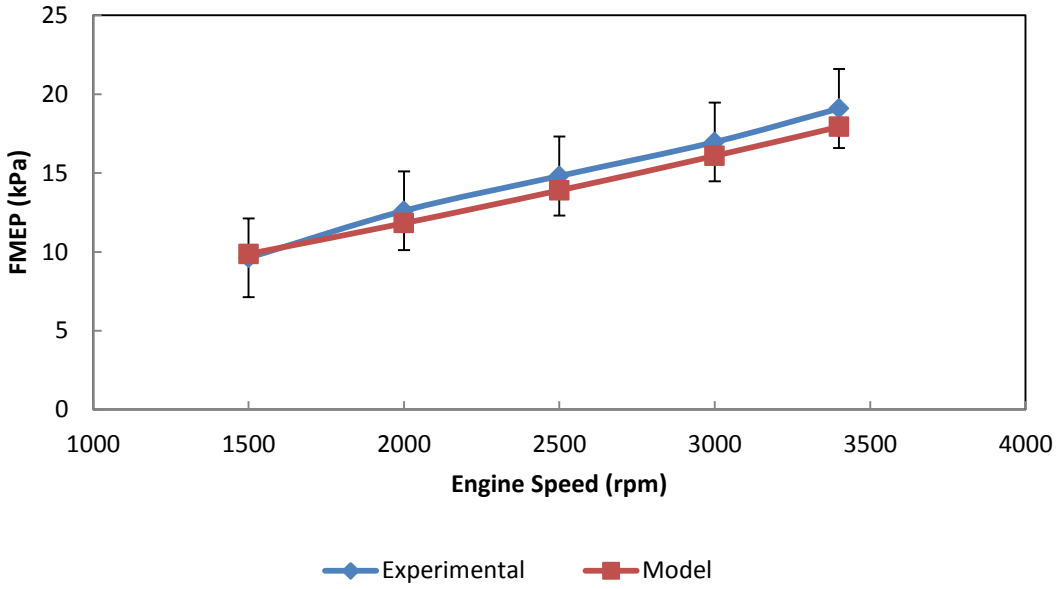

Figure 4.5. An example of a data analysis plot

5. RESULTS FOR ENGINE 1

5.1. BREAKDOWN TEST RESULTS

As described in the previous section, a breakdown motoring test was conducted on the Engine 1. The torque required to motor the engine at different configurations was recorded. The Frictional Mean Effective Pressure (FMEP) was calculated from the acquired motoring torque. The results of the test are shown in Figure 5.1. Clearly, as components are added to the engine the motoring torque also increases due to the increase in the number of rubbing surfaces. Additionally, frictional FMEP increases with engine speed due to the increase in relative velocity between the surfaces.

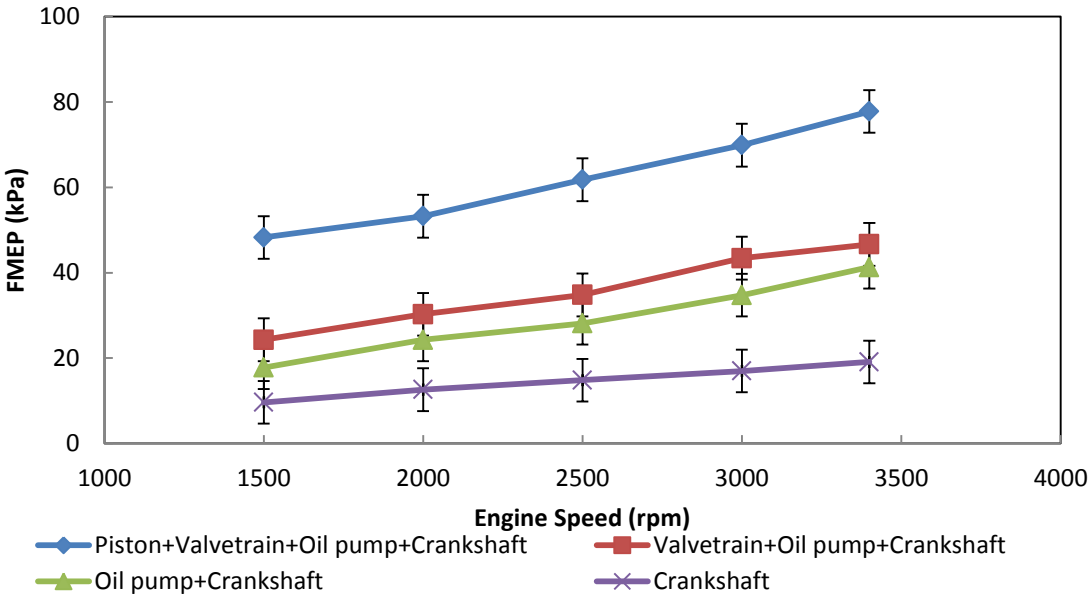

Figure 5.1. Motoring FMEP at different speeds

5.2. OIL AND TEMPERATURE VARIATION TEST RESULTS

Figures 5.2 to 5.7 show variation in total rubbing engine friction due to the change in viscosity and temperatures. The total rubbing friction is the sum of the friction contribution from the crankshaft, auxiliary, valvetrain and piston assembly. Six different grades of lubricating oils (SAE 5W20, SAE 10W30, SAE 10W40, SAE 30, SAE 40 and SAE 50) were used in the oil variation test. It is evident from the plots that at a given engine speed the total friction is higher at lower temperatures. This is due to the high viscosity of the lubricant at low temperatures.

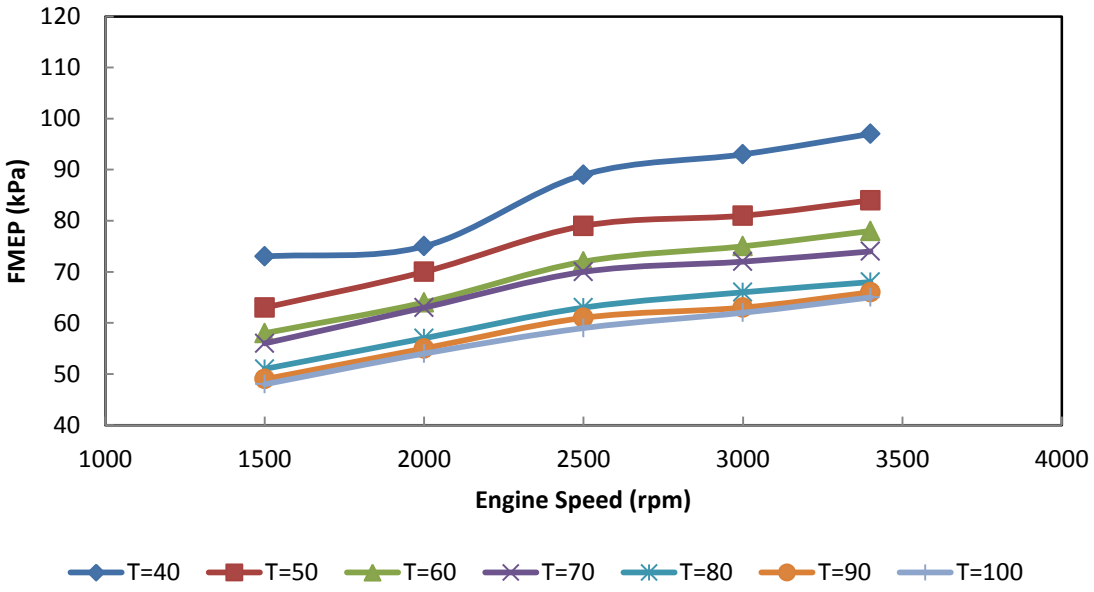

Figure 5.2. Motoring FMEP at different speeds and temperatures for SAE 5W20

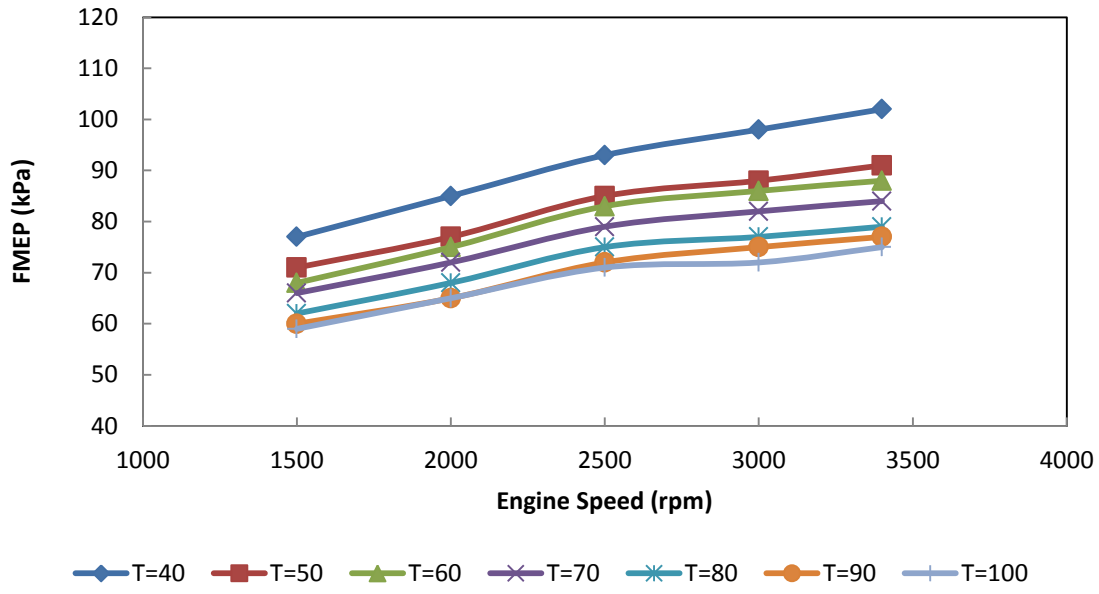

Figure 5.3. Motoring FMEP at different speeds and temperatures for SAE 10W30

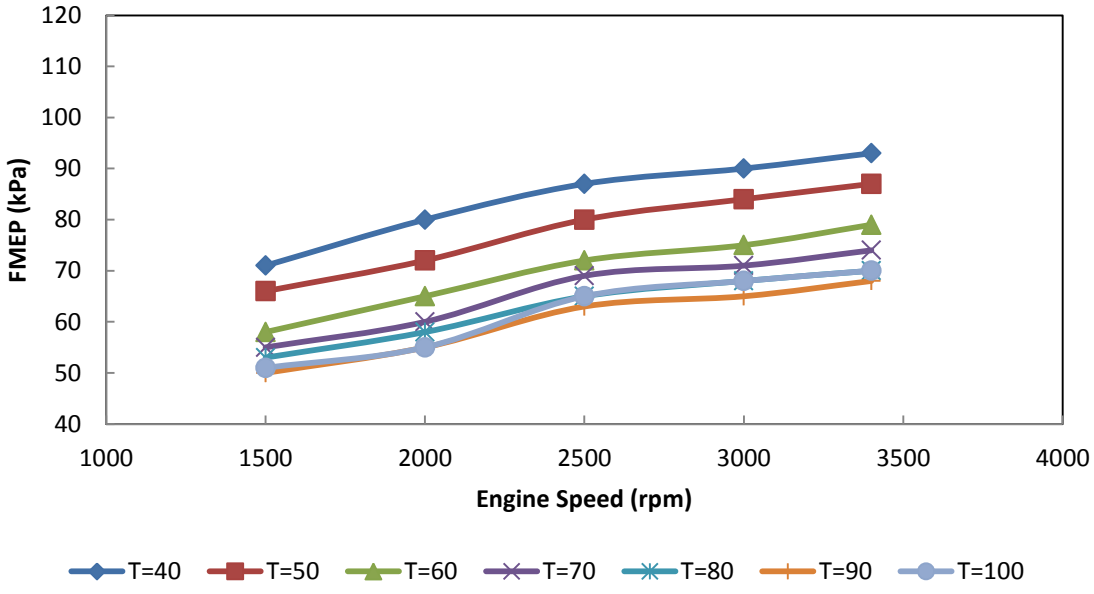

Figure 5.4. Motoring FMEP at different speeds and temperatures for SAE 10W40

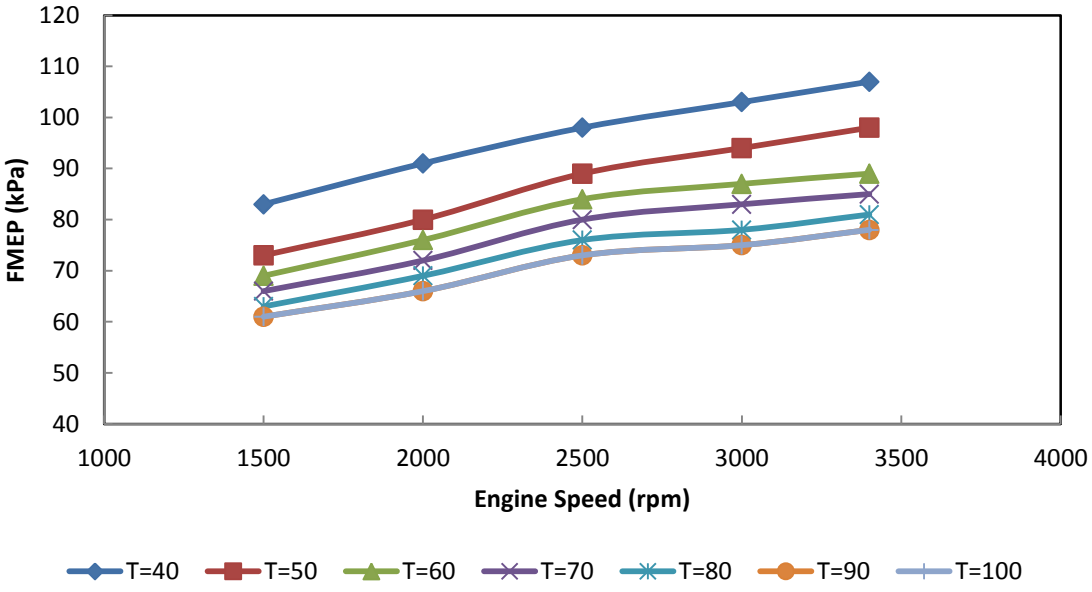

Figure 5.5. Motoring FMEP at different speeds and temperatures for SAE 30

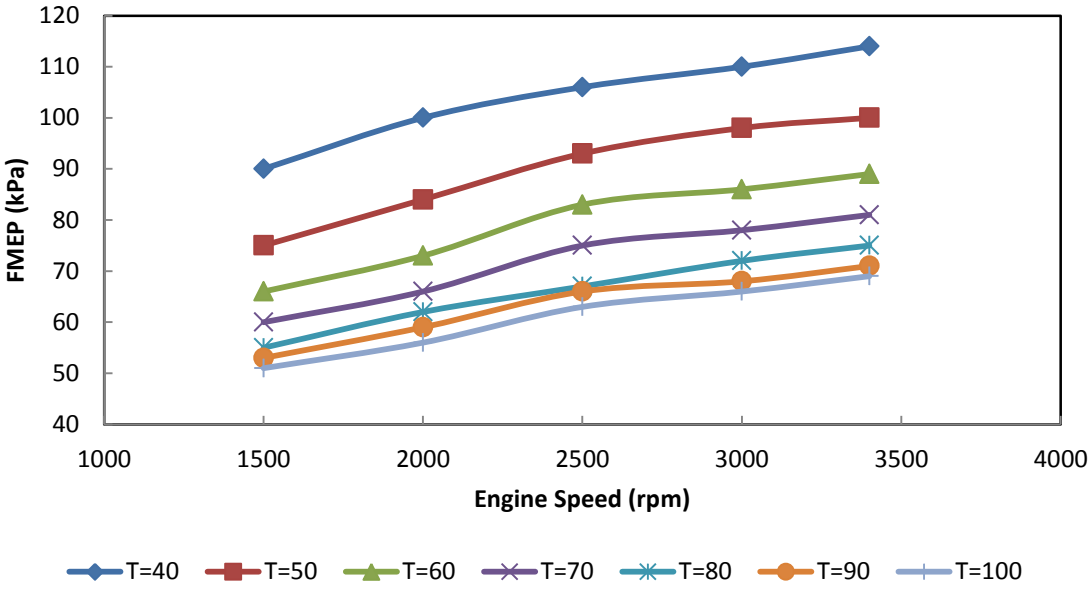

Figure 5.6. Motoring FMEP at different speeds and temperatures for SAE 40

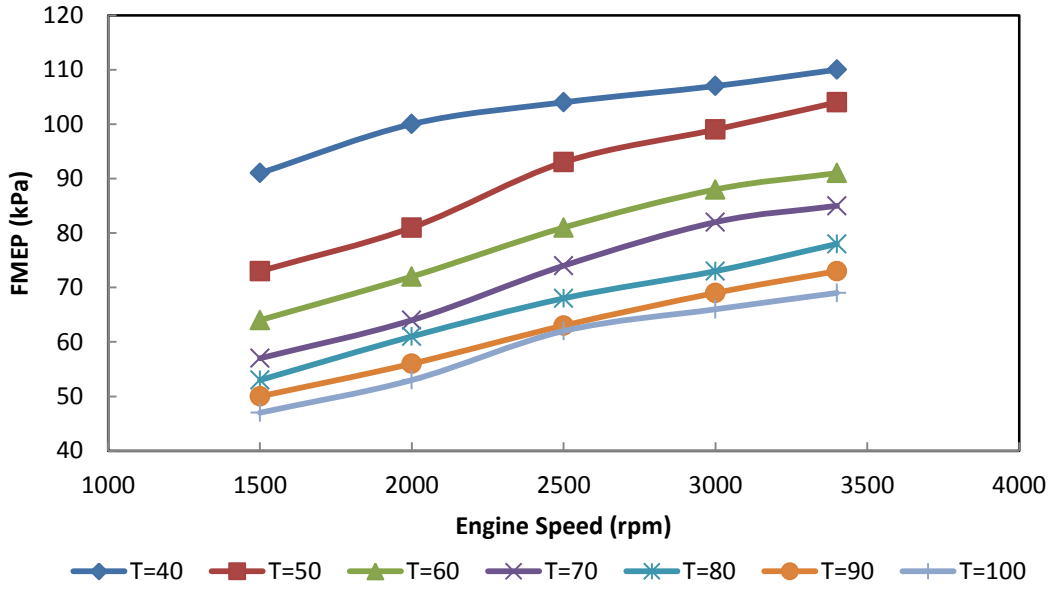

Figure 5.7. Motoring FMEP at different speeds and temperatures for SAE 50

Figures 5.2 to 5.7 show expected trends in the engine friction. It can be clearly observed that the FMEP increases with increasing engine speed. Also, as the temperature increases the engine friction decreases, this is due the decrease in the viscosity of the lubricant with increase in temperature.

6. MODEL DESCRIPTION AND MODIFICATION

The main approach used in the development of the PNH model was based on the basic friction calculation. The coefficient of friction was multiplied to the normal force to obtain the force of friction. The friction force was then multiplied to the velocity to obtain the frictional power. Since the engine has rotating parts the velocity was assumed to the product of the engine speed and the respective diameter of the part under consideration. The frictional power was then converted to FMEP by dividing it with the product of displacement volume and engine speed. Lastly, the FMEP terms were calibrated using the experimental results. Assumptions about the lubrication regimes and dimensional proportions were made for each term. The PNH model was applied to Engine 1. Figure 6.1 shows the predicted friction for the different sub-assemblies.

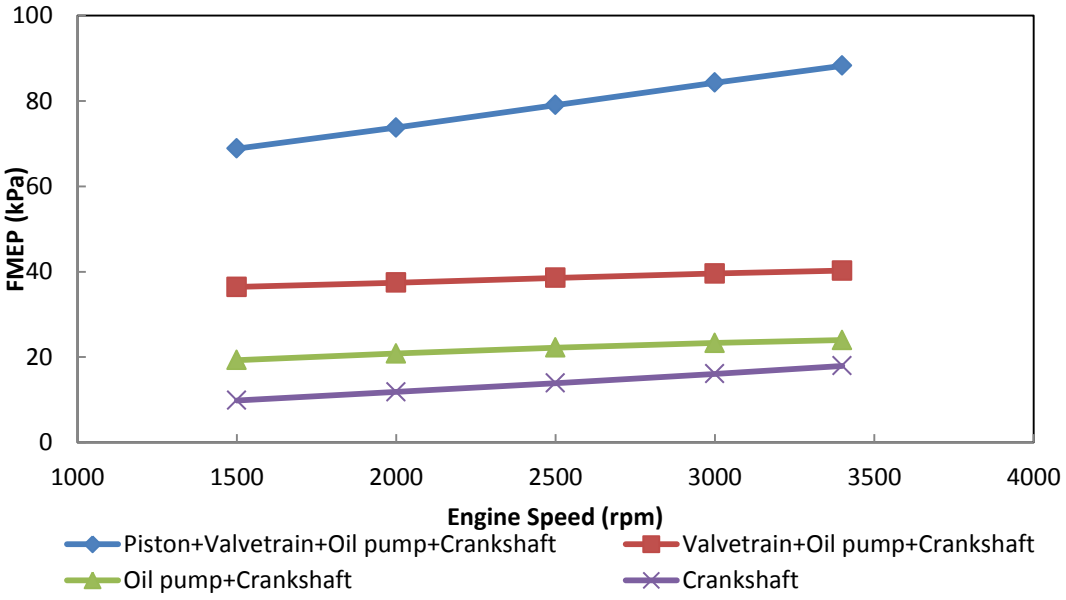

Figure 6.1. Model FMEP at different speeds

6.1. CRANKSHAFT FRICTION MODEL

6.1.1. Model Description. The crankshaft friction prediction model predicts the friction associated with the components of the crankshaft which mainly consist of the bearing seals and bearings. A turbulent dissipation was also included in the model to account for the losses due to the transport of the oil. The approach used in the PNH model derivation and modification of the prediction terms is described in detail below.

6.1.1.1 Bearing seal term. The boundary lubrication regime was assumed for the bearing seals in the PNH friction model. This assumption was based on the direct contact between the seal lip and the crankshaft surface. The normal force in the case of seal lip was assumed to be constant. The Figure 6.2 shows the bearing seal present on the test engines for this study.

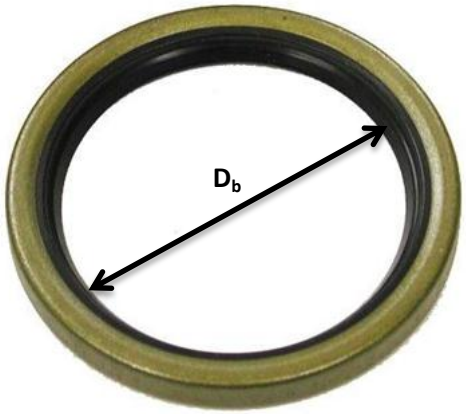

Figure 6.2. Bearing seal

The FMEP term was derived to be:

$$F_f = fF_n = \text{Constant} \tag{7}$$

$$P_f = F_f V \propto ND_b \tag{8}$$

$$\text{FMEP} \propto \frac{P_f}{NV_d} \propto \frac{ND_b}{NV_d} \propto \frac{D_b}{B^2 Sn_c} \tag{9}$$

The constant was found to be 1.22x105 kPa-mm^2. All the constants in the PNH model were determined using the data from the motoring breakdown tests from multiple engines (2). All the constants for each sub-assembly were determined together through a curve fit on the motoring data.

6.1.1.2 Main bearing hydrodynamic friction term. The term for the bearing friction was derived assuming the hydrodynamic lubrication regime due to the adequate oil supply to the bearings. The coefficient of friction is taken to be proportional to the duty parameter (Section 2.1.1). The bearing clearance, c, was assumed to be constant. A sleeve bearing is shown in Figure 6.3.

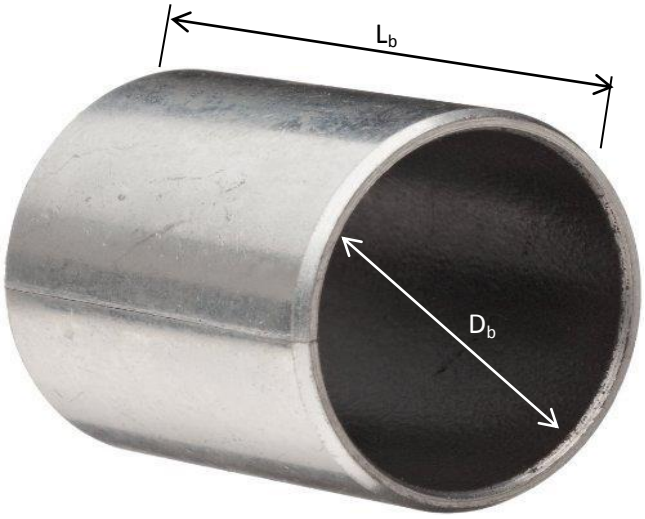

Figure 6.3. Sleeve bearing

The FMEP equation was found to be:

$$F_f = fF_n \propto \frac{\mu V A F_n}{F_n c} \propto VA \propto ND_b^2 L_b \tag{10}$$

$$P_f = F_f V n_b \propto ND_b^2 L_b ND_b L_b \propto N^2 D_b^3 L_b n_b \tag{11}$$

$$FMEP \propto \frac{P_f}{NV_d} \propto \frac{N^2 D_b^3 L_b n_b}{NB^2 Sn_c} \propto \frac{ND_b^3 L_b n_b}{B^2 Sn_c} \tag{12}$$

The above given term for the main bearing hydrodynamic friction can be derived from the concept of a rotating cylinder viscometer which shears the fluid in a narrow clearance. The Figure 6.4 describes the viscometer.

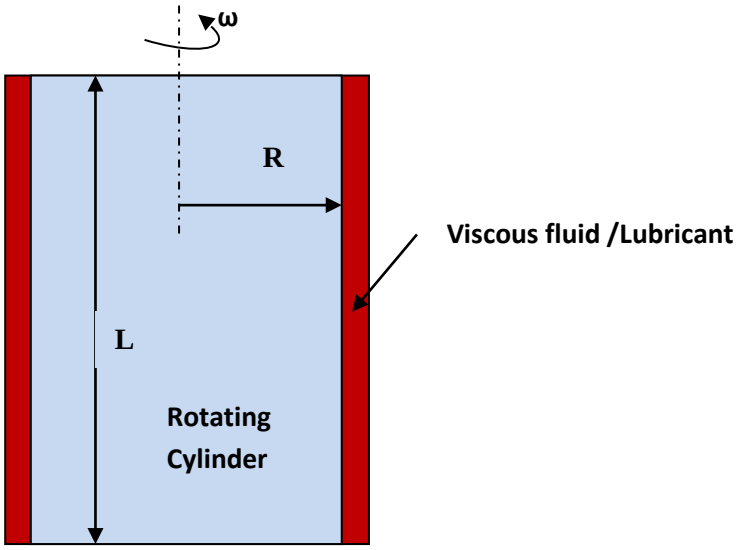

Figure 6.4. Rotating cylinder viscometer

Analyzing the annular region (Curved surface of the cylinder). The shear stress is given by the Newton's law of viscosity.

$$\tau=\mu\frac{du}{dy}=\mu\frac{\omega R}{\Delta R} \tag{13}$$

Therefore, the torque (T) due to the shear force which is normal to the radius is given by

$$T=\int R.dF=\int R\tau\omega.dA=\int_0^{2\pi}\frac{R\mu\omega}{\Delta R}RLd\theta=\frac{2\pi\mu\omega R^3L}{\Delta R} \tag{14}$$

The relationship between Frictional Mean Effective Pressure (FMEP) and torque is given by the equation below.

$$FMEP=\frac{2\pi n_r T}{V_d} \tag{15}$$

T is substituted into the Equation 14 to get the equation of the FMEP.

$$FMEP=\frac{2\pi n_r}{V_d}\frac{2\pi\mu\omega R^3L}{\Delta R}=\frac{2\pi n_r}{\pi\left(B^2/_4\right)S}\frac{2\pi\mu}{\Delta R}\frac{N}{2\pi}\frac{D_b^3}{8}L_b=\frac{\mathbf{\mu n_r}}{\mathbf{\Delta R}}\frac{\mathbf{ND_b^3L_b}}{\mathbf{B^2S}} \tag{16}$$

The derivation from the rotating viscometer concept gives the coefficient ($\mu n_r/\Delta R$) for the main bearing term. Due to the small order of magnitude ($3.23x10^{-4}$) of

the constant term and to maintain the broad view of the model, the constant was determined using the curve fit on the experimental data (2) of the PNH model . The constant for the main bearing hydrodynamic term was 3.03×10^{-4} kPa-min/rev-mm (2), used in the PNH model

6.1.1.3 Turbulent dissipation term. The turbulent dissipation is the work required to pump fluids through a restriction. So, it was assumed to be relative to the pressure drop across the bearing. According to Bernoulli's equation the pressure drop is proportional to the product of density of the fluid and the square of the velocity. The velocity is proportional to $D_b N$.

$$FMEP \propto \frac{D_b^2 N^2 n_b}{n_c} \tag{17}$$

Hence, the constant for turbulent dissipation term was 1.35×10^{-10} kPa-mm^2. All constants for the bearing seal, main bearing and the turbulent dissipation terms were determined simultaneously through a curve fit on the motoring test data (2). Note: the number of bearings (n_b) is one plus one half the number of cylinders (n_c) in a V- engine.

6.1.2. Results. The PNH model predicted the crankshaft friction with acceptable accuracy, concluded from the Figure 6.5 The error bar depicts the instrumental uncertainty of the torque transducer. No modifications were made to the crankshaft friction terms of the PNH model. Same constants were used as given by the PNH model. The complete crankshaft friction prediction term is give below. The subscript for each term denotes the part of the sub-model (eg. BST is the Bearing Seal Term).

$$\text{FMEP(kPa)}=\left(1.22\times10^{5}\left(\frac{D_b}{B^2Sn_c}\right)\right)_{\text{BST}}+\left(3.03\times10^{4}\frac{ND_b^3L_bn_b}{B^2Sn_c}\right)_{\text{MBHT}}+\left(1.35\times10^{-10}\left(\frac{D_b^2N^2n_b}{n_c}\right)\right)_{\text{TDT}} \quad (18)$$

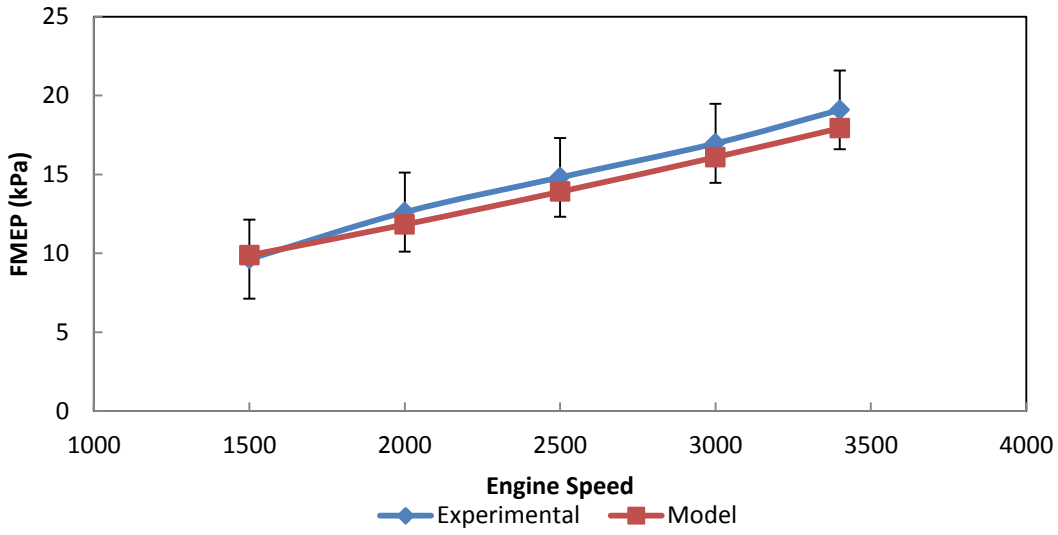

Figure 6.5. Experimental vs. model friction for the crankshaft

6.2. ACCESSORY FRICTION MODEL

6.2.1. Model Description. Auxiliary friction comprises of accessories like oil pump, water pump and non-charging alternator friction. The FMEP can be expressed in terms of engine speed. The PNH model assumed all auxiliary power losses to be proportional to engine displacement. Since FMEP is a per unit volume quantity, the auxiliary losses can be expressed in terms engine speed. The oil pump was the only auxiliary component present in the Engine 1 and Engine 2.

$$FMEP=C_1+C_2N+C_3N^2 \quad (19)$$

6.2.2. Results. The initial comparison between the original model and the experimental results is shown in Figure 6.6. The original PNH model for the accessory friction was just based on a curve fit of the data from automotive-type engines. Clearly, the PNH model under predicts the oil pump friction of the Engine 1 engine. This requires the model to be modified to predict the oil pump friction more accurately.

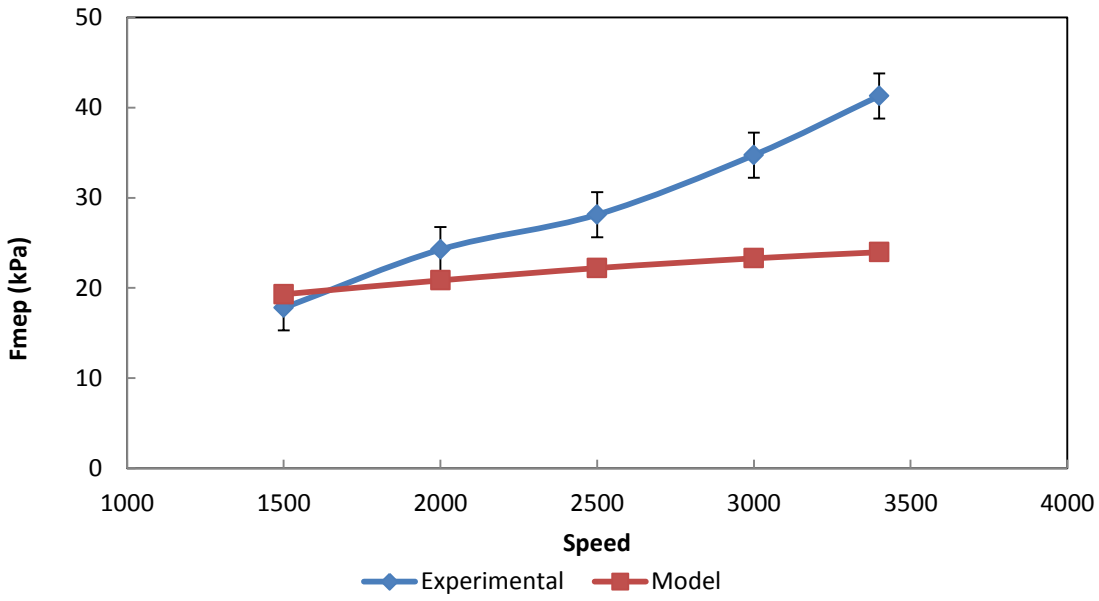

Figure 6.6. Experimental vs. model friction for crankshaft and oil pump

6.2.3. Modifications. The oil pump friction loss of the Engine 1 was analyzed using the steady flow energy equation. The following assumptions were made to derive the work of the oil pump.

i. No heat energy is supplied or taken away from the pump.

ii. Flow of the oil is steady at the inlet and outlet of the pump.

iii. The change in elevation of the oil was neglected because the outlet of the pump is close to the inlet.

iv. The density of the oil was assumed to be constant.

According to Reynold's transport theorem:

$$\left.\frac{dB}{dt}\right|_{system} = \frac{d}{dt}\int B\rho d\forall + \int B\rho\vec{V}.d\vec{A} \tag{20}$$

$$\dot{q}+\dot{w}_{shaft} = \frac{d}{dt}\int\left(u_i+\frac{V^2}{2}+gz\right)\rho d\forall + \int\left(h+\frac{V^2}{2}+gz\right)\rho\vec{V}.d\vec{A} \tag{21}$$

As the control volume under consideration does not change with time, the time derivative term equals to zero. In addition to no change in control volume it is also assumed that the change in elevation between the inlet and the outlet of the pump is negligible. As Enthalpy, h, in Equation 21 is substituted by $\Delta P/\rho$.

$$\dot{w}_{shaft} = \left(\frac{P_2\text{-}P_1}{\rho}+\frac{V^2}{2}\right).\rho\vec{V}.\vec{A} \tag{22}$$

The results from this analysis revealed that the friction loss from the pump was directly proportional to the sum of the pressure drop across the pump and the square of

the engine speed as the oil flow scaled directly with the engine speed. The pump work when described in terms of FMEP means the work done by the pump per cycle per unit displaced volume of the engine. Results from this new model have been shown in Figure 6.7, in comparison with the experimental results.

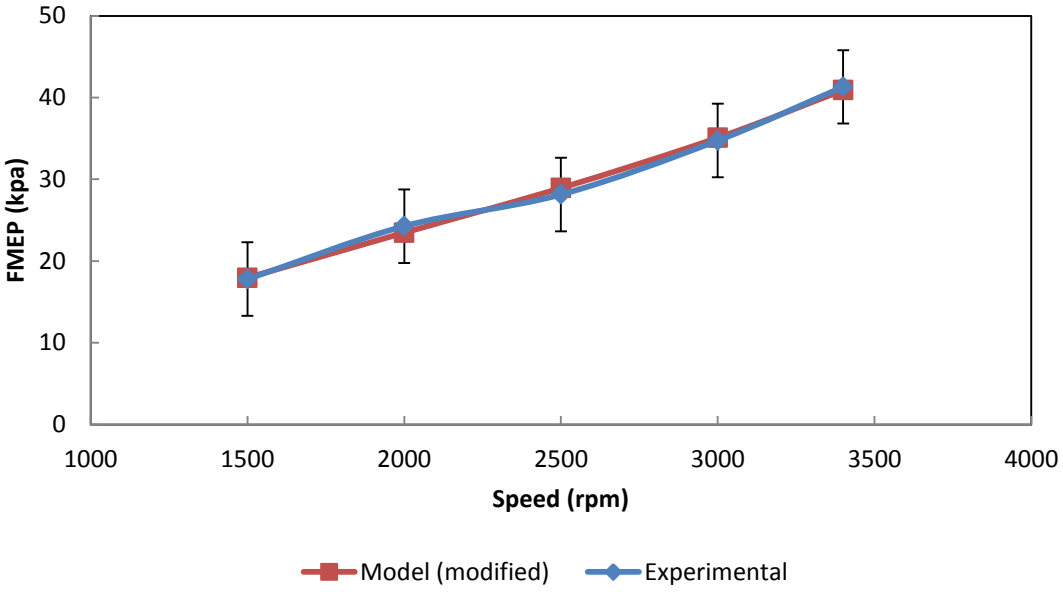

Figure 6.7. Experimental vs. modified model friction for crankshaft and oil pump

Results from lab tests suggest that a variation in the oil pressure difference, within the typical operating pressure difference range (60-90psi) of an oil pump, creates a very small change in the FMEP. Therefore, the pressure difference term was assumed to be a constant which was equal to 5.06 (derived from comparison with the motoring breakdown test). It is important to notice that 5.06 is the value for the whole pressure

difference term. The final equation for the accessory friction prediction term is given below.

$$FMEP(kPa)=5.06+\left(0.00000145\times N^2\right) \tag{23}$$

6.3. VALVETRAIN FRICTION MODEL

6.3.1. Model Description. The main contributors of the valvetrain friction are the camshaft, cam follower and the valve actuation mechanism. The terms which were used in the model are for camshaft bearing hydrodynamic friction, cam follower friction, oscillating hydrodynamic friction and oscillating mixed lubrication friction. The reason behind using both mixed and hydrodynamic oscillating terms is to capture the friction in the components with both mixed and hydrodynamic lubrication. Therefore, the frictional behavior of some valvetrain components is captured by a combination of both the mixed and the hydrodynamic lubrication terms. It was observed (2) that some part of the camshaft friction was independent of speed. This conclusion was made based on the data (2) which showed decrease in valvetrain friction with increase in engine speed. As the friction theoretically increases with speed, so, a decrease in friction with increase in speed proves that the friction is speed independent. A constant was added to the bearing friction term. This constant represents the friction from the bearing seals.

6.3.1.1 Camshaft bearing hydrodynamic friction term. The camshaft bearing term is same as that for the previous bearing terms in Section 6.1.1.2.

$$FMEP=\frac{Nn_b}{B^2Sn_c} \tag{24}$$

The constant was found to be $2.44x10^2$ kPa-mm^2 (2).

6.3.1.2 Flat follower friction term. Figure 6.8 shows a flat follower assembly over the cam lobe. Mixed lubrication regime exists between these two surfaces due to varying contact velocity. The normal force for the cam follower term was assumed in the PNH model to be proportional to the product of mass of the valvetrain and acceleration. The mass of the valve was assumed to be proportional to the square of the bore by the PNH model (2). Since the bore area is proportional to the valve area which in turn can be related to the mass of the valve.

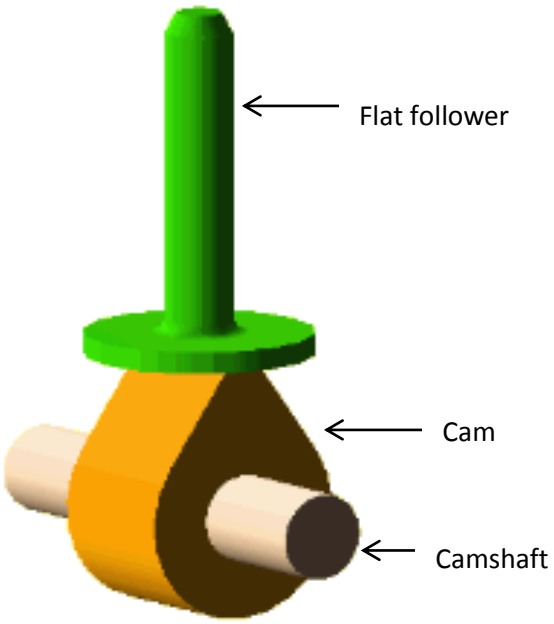

Figure 6.8. Flat follower assembly

The friction coefficient was assumed to be proportional to (1+1000/N) which is a function of engine speed. The model is given below.

$$F_f = fF_n \propto \left(1+\frac{1000}{N}\right) B^2 \tag{25}$$

$$P_f = F_f V n_v \propto \left(1+\frac{1000}{N}\right) B^2 N n_v \tag{26}$$

$$FMEP \propto \frac{P_f}{NV_d} \propto \left(1+\frac{1000}{N}\right)\frac{B^2 N n_v}{B^2 S N n_c} \propto \left(1+\frac{1000}{N}\right)\frac{n_v}{S n_c} \tag{27}$$

A roller cam follower term was also designed for engines with a roller follower. The roller cam follower friction (Equation 28) term is based on the assumption that the coefficient of friction was proportional to the engine speed. The Engine 1 and Engine 2 were not equipped with a roller cam. The roller cam follower term was the part of the PNH model, it was not used in this study. The term is as follows:

$$\frac{N n_v}{S n_c} \tag{28}$$

6.3.1.3 Oscillating hydrodynamic friction term. Both the oscillating hydrodynamic and mixed lubrication terms are used to model the respective lubrication regimes existing in multiple valvetrain components. These components have both types of lubrication regimes due to their oscillating nature. The oscillating hydrodynamic friction term is used to predict the portion of the hydrodynamic friction present between the valvetrain components. For instance, valve lifters and valve in the valve guide. In this

model the coefficient of friction was considered to be proportional to the square root of the duty parameter based on a study by Cameron (8). The mean valve speed was found to be proportional to the maximum valve lift (L_v) and engine speed.

$$F_f = fF_n \propto \left(\frac{\mu VL}{F_n}\right)^{0.5} F_n \propto (VLF_n)^{0.5} \tag{29}$$

$$P_f = F_f V n_v \propto \left(L_v N B^2\right)^{0.5} L_v N n_v = (L_v N)^{1.5} B n_v \tag{30}$$

$$FMEP \propto \frac{P_f}{NV_d} \propto \frac{(L_v N)^{1.5} B n_v}{B^2 S N n_c} = \frac{L_v^{1.5} N^{0.5} n_v}{B S n_c} \tag{31}$$

6.3.1.4 Oscillating mixed lubrication friction term. An oscillating mixed lubrication term was used to model the friction for the mixed lubricated interfaces of the valvetrain. Since an oscillating motion involves change in speed this results in some amount of boundary regime friction. This led to the assumption of mixed lubrication. The interaction of the pushrod at both ends, the rocker arm with the valve tip and valve stem and valve guide fall under the mixed lubrication regime. The term derived for the prediction is as follows.

$$F_f = fF_n \propto \left(1 + \frac{1000}{N}\right) B^2 \tag{32}$$

$$P_f = F_f V n_v \propto \left(1 + \frac{1000}{N}\right) B^2 L_v N n_v \tag{33}$$

$$FMEP \propto \frac{P_f}{NV_d} \propto \left(1 + \frac{1000}{N}\right) \frac{B^2 L_v N n_v}{B^2 S N n_c} \propto \left(1 + \frac{1000}{N}\right) \frac{L_v n_v}{S n_c} \tag{34}$$

6.3.2. Results. In comparison, the PNH model with the experimental results it becomes clear that the model over predicts. This observation from Figure 6.9 solidifies the need for a modification.

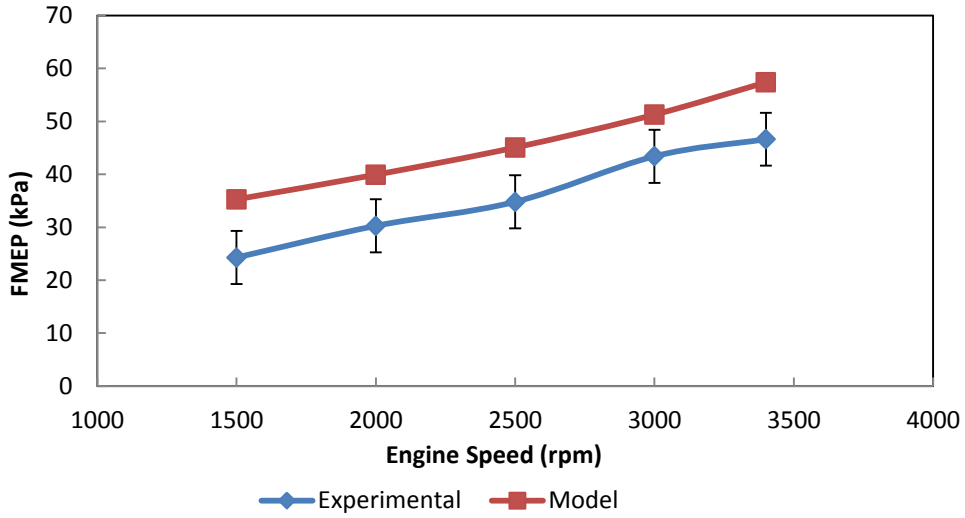

Figure 6.9. Experimental vs. model friction for crankshaft, oil pump and valvetrain

6.3.3. Modifications. There were two modifications made to the PNH model. In the first one, the constant bearing seal term was omitted from the camshaft bearing term. The reason behind removing the bearing seal term was that the engine under study did not contain any bearing seals. The second modification was to include the valve spring constant in the flat follower and the oscillating mixed friction term, as the compression of the spring decides the normal force on the follower surface. The PNH model assumes the normal force due to the spring to be proportional to the square of the bore. In case of small engines the square of the bore is significantly larger than the actual normal force

produces by the compression of the spring. The spring constant was determined using a compression test on the universal testing machine which was found to be 12.84 kN/m. The equations below show the modification for the flat follower term.

$$F_f = fF_n \propto \left(1 + \frac{1000}{N}\right) kL_v \tag{35}$$

$$P_f = F_f V n_v \propto \left(1 + \frac{1000}{N}\right) kL_v N n_v \tag{36}$$

$$FMEP \propto \frac{P_f}{NV_d} \propto \left(1 + \frac{1000}{N}\right) \frac{kL_v N n_v}{V_d N} \propto \left(1 + \frac{1000}{N}\right) \frac{kL_v n_v}{V_d} \tag{37}$$

Equations 38 to 40 describe the modification of the oscillating mixed lubrication terms.

$$F_f = fF_n \propto \left(1 + \frac{1000}{N}\right) kL_v \tag{38}$$

$$P_f = F_f V n_v \propto \left(1 + \frac{1000}{N}\right) kL_v^2 N n_v \tag{39}$$

$$FMEP \propto \frac{P_f}{NV_d} \propto \left(1 + \frac{1000}{N}\right) \frac{kL_v^2 n_v}{V_d} \tag{40}$$

Results from the model after these modifications are plotted in Figure 6.10. The complete valvetrain friction prediction term is listed in Equation 41. This equation consists of terms associated with the flat follower friction, the oscillating hydrodynamic friction, oscillating mixed friction and friction due to the camshaft bearings.

$$FMEP(kPa)=\left(244\frac{Nn_b}{B^2Sn_c}\right)_{MBHT}+\left(1.81\times10^{-2}\left(1+\frac{1000}{N}\right)\frac{kL_vn_v}{V_d}\right)_{FFT}$$
$$+\left(0.5\frac{L_v^{1.5}N^{0.5}n_v}{BSn_c}\right)_{OHLT}+\left(\left(1+\frac{1000}{N}\right)\frac{kL_v^2n_v}{V_d}\right)_{OMLT} \quad (41)$$

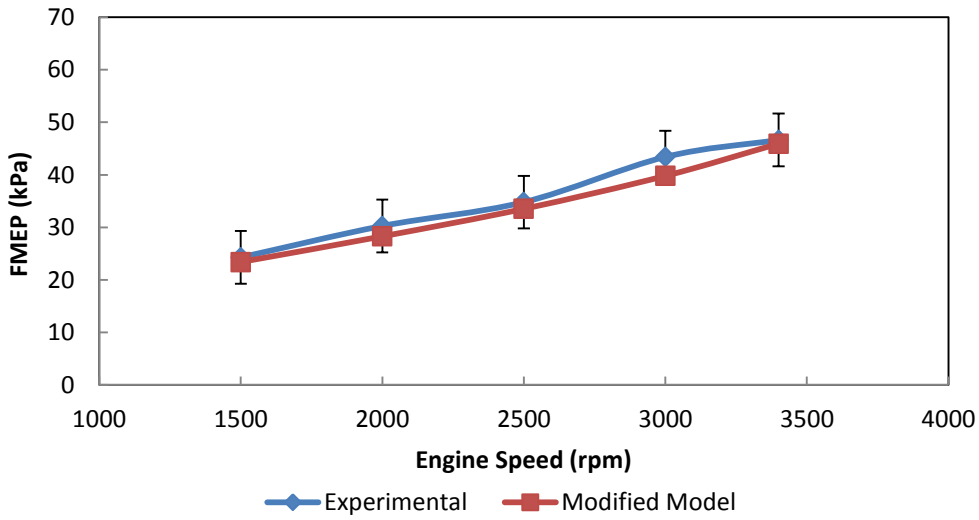

Figure 6.10. Experimental vs. modified model friction for crankshaft, oil pump and valvetrain

6.4. RECIPROCATING FRICTION MODEL

6.4.1. Model Description. The contributors to the reciprocating friction are piston, piston rings and the connecting rod. Experiments in the past (9) suggests that the combination of both boundary and hydrodynamic friction is present in the piston friction. The friction is maximum at during the middle portion of the stroke, this part of the friction falls under hydrodynamic regime. The boundary lubrication occurs at the end of the stroke, i.e. when the direction of the piston is reversed. Boundary and hydrodynamic

friction is always present in oscillating assemblies which involves quick change in the direction of motion. Figure 6.11 shows a typical piston assembly.

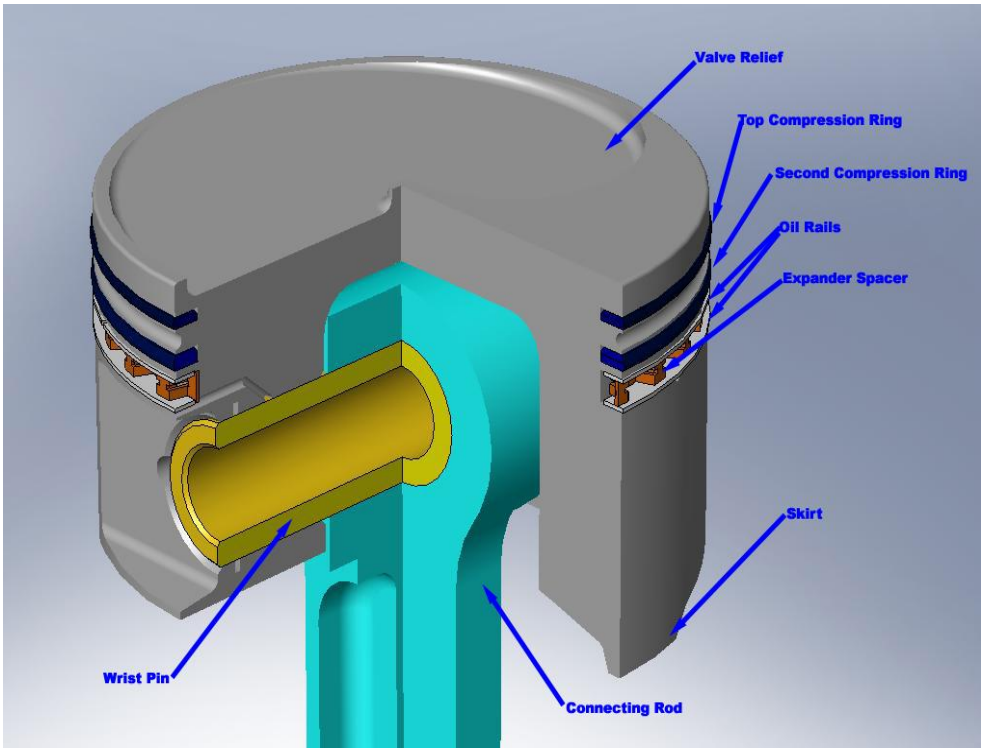

Figure 6.11. Piston assembly

It consists of two compression rings which seal the gases inside the cylinder and prevent them from escaping to the crankcase. The third ring is the oil ring which helps in the circulation of the lubricating oil through the cylinder walls. The region below the oil rings is called the piston skirt.

6.4.1.1 Reciprocating friction term. The reciprocating friction model was developed assuming hydrodynamic lubrication regime. This term accounts for the

hydrodynamic lubrication of the piston assembly. The ring friction is modeled based on mixed lubrication to account for boundary regime at the end of the stroke. The skirt length was assumed to be proportional to the bore. The piston friction term is as follows:

$$F_f = fF_n \propto \frac{\mu V L_s F_n}{F_n} \propto \mu V L_s \tag{42}$$

$$P_f = F_f V \propto S_p^2 B \tag{43}$$

$$FMEP \propto \frac{P_f}{NV_d} \propto \frac{S_p^2 B}{B^2 SN} \propto \frac{S_p^2 B}{B^2 S_p} \propto \frac{S_p}{B} \tag{44}$$

In the above mentioned equation the constant of proportionality was found to be 2.94×10^2kPa-mm-s/m (2). This constant was derived simultaneously with the constants for the connecting rod bearing term and the term for the piston rings without the gas pressure loading using the data from the motoring breakdown test.

6.4.1.2 Piston ring friction term without gas pressure loading. The ring friction term without the gas pressure loading was developed assuming the mixed lubrication regime. An empirical function based on engine speed was used to model the decrease in friction. The normal force was assumed to be constant due to absence of pressure loading.

$$F_f = fF_n \propto \left(1 + \frac{1000}{N}\right) \times \text{constant} \tag{45}$$

$$P_f = F_f V \propto \left(1 + \frac{1000}{N}\right) S_p \tag{46}$$

$$FMEP \propto \frac{P_f}{NV_d} \propto \left(1+\frac{1000}{N}\right)\frac{S_p}{B^2SN} \propto \left(1+\frac{1000}{N}\right)\frac{1}{B^2} \quad (47)$$

6.4.1.3 Gas pressure loading term. The term modeled for the increase in friction due to the gas pressure loading used intake pressure and compression ratio to predict the friction it was developed by Bishop from the fired friction data (9). The compression ratio has an exponent of 1.3 (related to the physics of the compression process) which reduces with the increase in the mean piston speed. The whole process was considered to be in the mixed lubrication regime. The term is given as follows.

$$FMEP = 6.89\frac{P_i}{P_a}\left[0.088r_c + 0.182r_c^{(1.33-KS_p)}\right] \quad (48)$$

6.4.1.4 Hydrodynamic journal bearing term. This term is the same as the one used in Equation 12 for the crankshaft main bearing term.

6.4.2. Results. Comparison of PNH model with the experimental results: The Figure 6.12 shows that the PNH model over predict the piston group friction. They over-prediction by the PNH model may be due the fact that the PNH model was designed for large automotive engines and it cannot effectively capture the friction associated with small SI engines. Therefore, there is a need for modification.

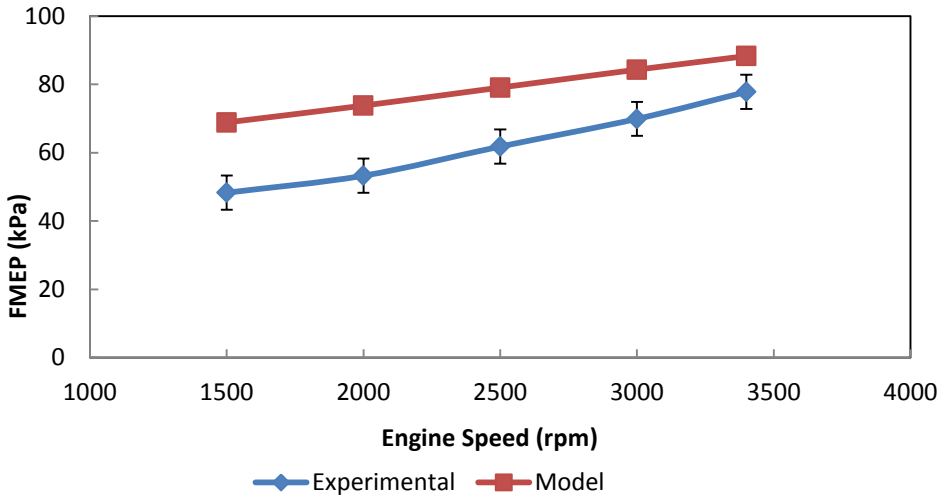

Figure 6.12. Experimental vs. model friction for crankshaft, oil pump, valvetrain and piston group

6.4.3. Modifications. The PNH model initially assumed that the piston skirt length was proportional to the bore. This assumption was suspended and the actual skirt length was used in the piston friction term. This assumption holds good for larger engines but for smaller engine, like Engine 1 the bore diameter and actual skirt length differ by approximately 68%. The large difference in the fundamental designs of large and small engines causes the PNH model to over predict. The modified model was applied to the test engine; the results are plotted in the Figure 6.13. The full equation for the piston assembly friction prediction term is given below.

$$\mathrm{FMEP(kPa)}=\left(294\left(\frac{S_p L_s}{B^2}\right)\right)_{\mathrm{PST}}+\left(4.06\times10^4\left(1+\frac{1000}{N}\right)\frac{1}{B^2}\right)_{\mathrm{PRFT}}$$
$$+\left(3.03\times10^4\frac{ND_b^3L_bn_b}{B^2Sn_c}\right)_{\mathrm{HJBT}}+\left(6.89\frac{P_i}{P_a}\left[0.088r_c+0.182r_c^{(1.33-KS_p)}\right]\right)_{\mathrm{GPLT}} \quad (49)$$

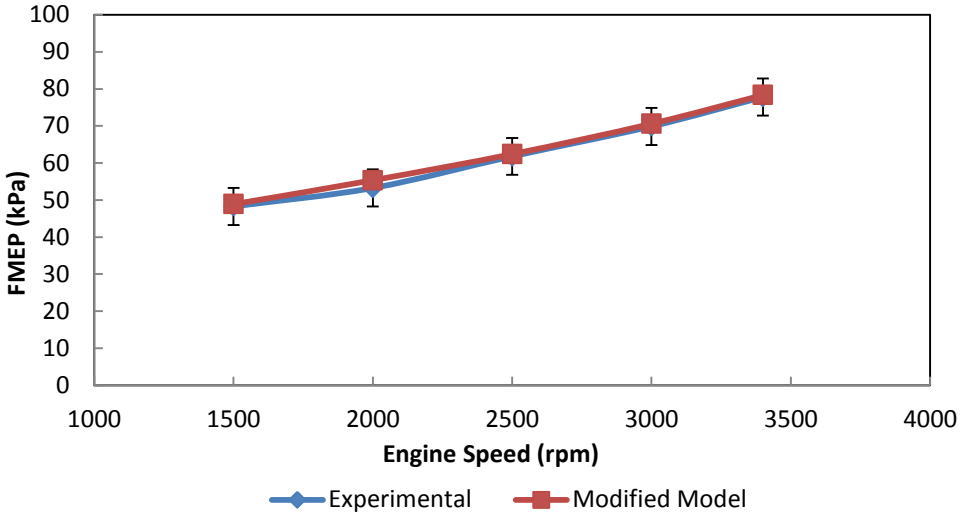

Figure 6.13. Experimental vs. modified model friction for crankshaft, oil pump, valvetrain and piston group

6.5. INTRODUCTION OF VISCOSITY SCALING IN THE MODIFIED PNH MODEL

6.5.1. Concepts of Viscosity Scaling. The PNH model did not account for any change in the viscosity of the lubricating oil with change in temperature. The literature showed (4) that Vogel's equation predicts the change in viscosity of the oil with changing temperature. Vogel's equation is a relationship between the low shear kinematic viscosity and oil temperature.

$$\nu = k \exp\left(\frac{\theta_1}{\theta_2 + T}\right) \tag{50}$$

Where ν is the low shear rate viscosity of the oil (i.e. the viscosity of the lubricant at low shear/low load conditions), T is the oil temperature and k and ϴ are the correlation constants for oil. These correlation constants in Equation 50 are derived from the known viscosity and temperature data for different oils. At least three known viscosities at corresponding temperatures should be known for calculating Θ_1, Θ_2 and k (three equations and three variables). Previously, it has been proven (10) that the dynamic viscosity scaling, μ, in hydrodynamic regime should be of the form represented in equation 51.

$$\mu_{Scaling}=\sqrt{\frac{\mu(T)}{\mu_0(T_0)}} \tag{51}$$

The low shear rate viscosity was then multiplied with a ratio of μ_∞/μ_o to convert to high shear rate kinematic viscosity. Large numbers of engine components operate at high shear rate. Most engines operate in the high shear viscosity range.

$$\nu=\nu_0\left(\frac{\mu_\infty}{\mu_0}\right) \tag{52}$$

Since ν and μ are related by just density, density was assumed to be constant (4). The viscosity scaling term which was applied to the model was of the form:

$$\mu_{Scaling} = \sqrt{\frac{\nu(T)}{\nu_0(T_0)}} \tag{53}$$

Where $\nu(T)$ is the viscosity for which the prediction has to be made and $\nu_0(T_0)$ is the known viscosity of the oil at which the model was calibrated.

6.5.2. Application of Viscosity Scaling to the Modified PNH Model. The PNH model results were based on the viscosity of the oil 10W30 at 90^{o}C. Therefore, the Vogel's equation was calibrated at 90^{o}C for the purpose of this study. The different components of the PNH model after the application of the viscosity scaling are given below. It should be noted that the viscosity scaling can only be applied to the terms with hydrodynamic friction.

6.5.2.1 Crankshaft friction model.

$$FMEP(kPa) = \left(1.22\times10^{5}\left(\frac{D_b}{B^2Sn_c}\right)\right)_{BST} + \left(3.03\times10^{4}\sqrt{\frac{\mu}{\mu_0}}\frac{ND_b^3L_bn_b}{B^2Sn_c}\right)_{MBHT} + \left(1.35\times10^{-10}\left(\frac{D_b^2N^2n_b}{n_c}\right)\right)_{TDT} \tag{54}$$

6.5.2.2 Accessory friction model. Since the accessory friction was mainly dependent mainly on the speed, the viscosity scaling was not applied to the accessory model.

6.5.2.3 Valvetrain friction model.

$$FMEP(kPa) = \left(244\sqrt{\frac{\mu}{\mu_0}}\frac{Nn_b}{B^2Sn_c}\right)_{MBHT} + \left(1.81\times10^{-2}\left(1+\frac{1000}{N}\right)\frac{kL_vn_v}{V_d}\right)_{FFT}$$

$$+\left(0.5\sqrt{\frac{\mu}{\mu_0}}\frac{L_v^{1.5}N^{0.5}n_v}{BSn_c}\right)_{OHLT}+\left(\left(1+\frac{1000}{N}\right)\frac{kL_v^2n_v}{V_d}\right)_{OMLT} \quad (55)$$

6.5.2.4 Reciprocating friction model.

$$FMEP(kPa)=\left(294\sqrt{\frac{\mu}{\mu_0}}\left(\frac{S_pL_s}{B^2}\right)\right)_{PST}+\left(\left(1+\frac{1000}{N}\right)\frac{1}{B^2}\right)_{PRFT}$$

$$+\left(3.03\times10^4\sqrt{\frac{\mu}{\mu_0}}\frac{ND_b^3L_bn_b}{B^2Sn_c}\right)_{HJBT}+\left(6.89\frac{P_i}{P_a}[0.088r_c+0.182r_c^{(1.33-KS_p)}]\right)_{GPLT} \quad (56)$$

6.5.3. Comparison Between the Oil and Temperature Variation Test and Modified PNH Model Results. The comparison between the experimental results and modified PNH model between the temperature ranges 40^{o}C to 100^{o}C for Engine 1 is shown in the graphs below. The oil used was SAE 10W30. It can be clearly observed from the Figures 6.14 to 6.18 that the introduction of the viscosity scaling to the modified PNH model has made it capable of predicting friction with varying temperature and viscosity.

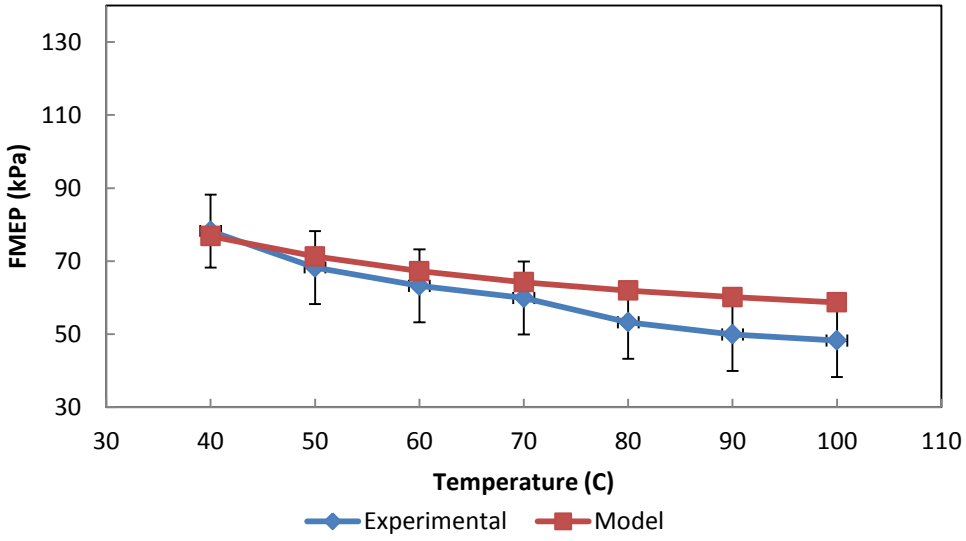

Figure 6.14. Model vs. experimental results for temperature variation at 1500 rpm

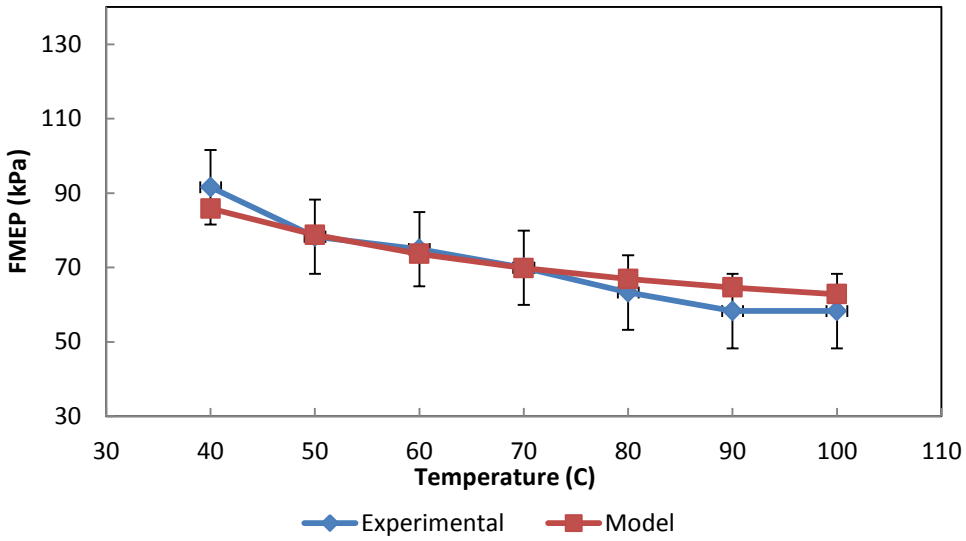

Figure 6.15. Model vs. experimental results for temperature variation at 2000 rpm

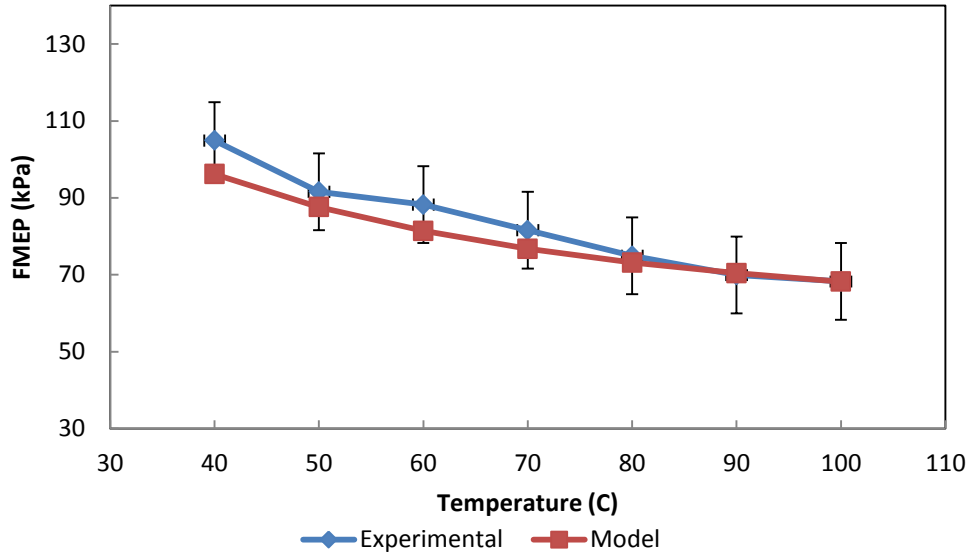

Figure 6.16. Model vs. experimental results for temperature variation at 2500 rpm

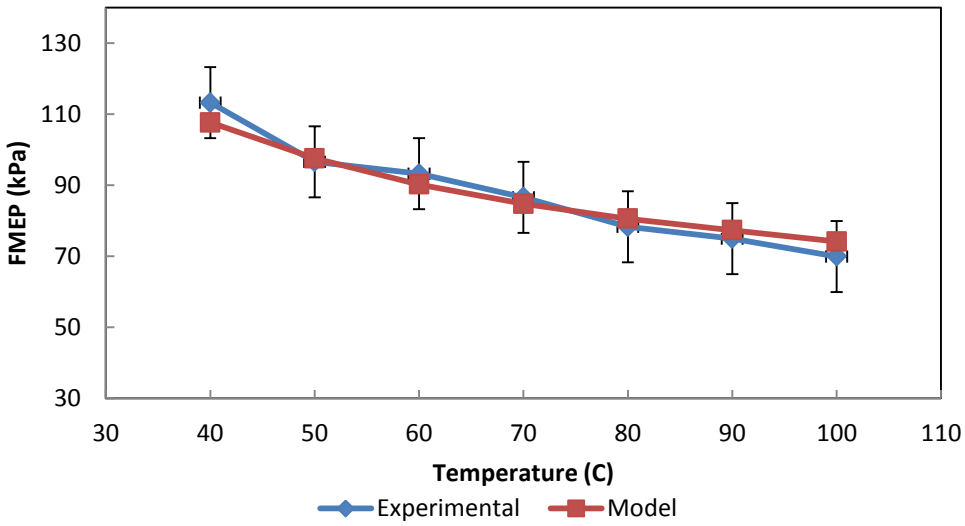

Figure 6.17. Model vs. experimental results for temperature variation at 3000 rpm

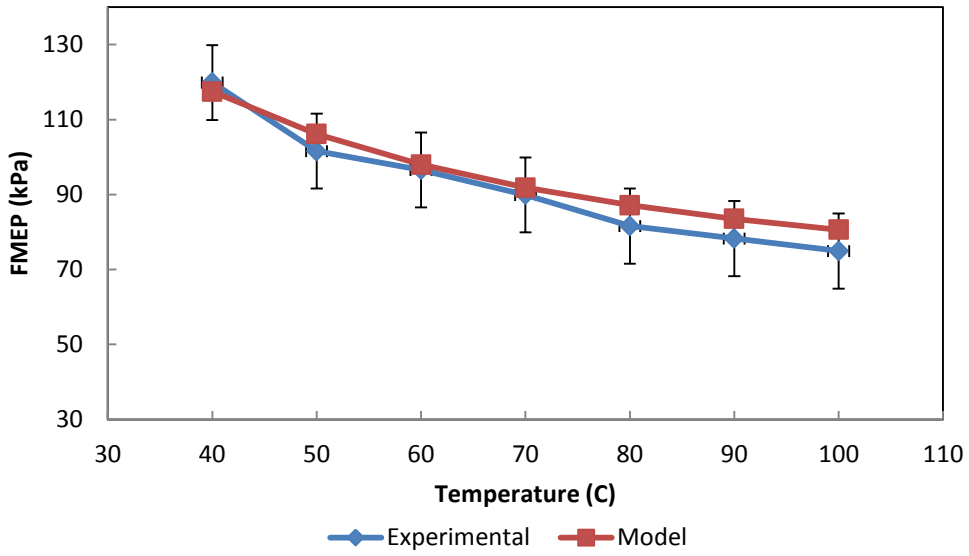

Figure 6.18. Model vs. experimental results for temperature variation at 3400 rpm

The comparison between the model and the experimental results for the different oils at 3000 rpm is given in Figures 6.19 to 6.23.

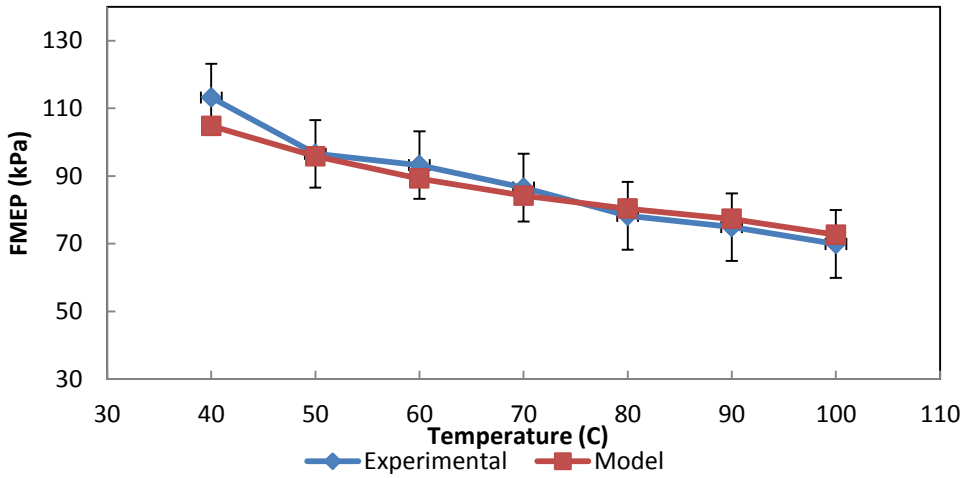

Figure 6.19. Model vs. experimental results for oil SAE 5W20 at 3000rpm

The figures above show that the modified PNH model is able to predict the variation in the rubbing friction with changing Oil viscosity. It can be observed (Figures 6.21, 6.22, 6.23) that the model slightly under predicts the rubbing friction at low temperatures. This is due presence for boundary and mixed lubrication at various surfaces in the engine. Due the high viscosity of the oil at low temperatures the flow of the oil to different rubbing surface in the engine is less, this leads to an increase in the rubbing friction.

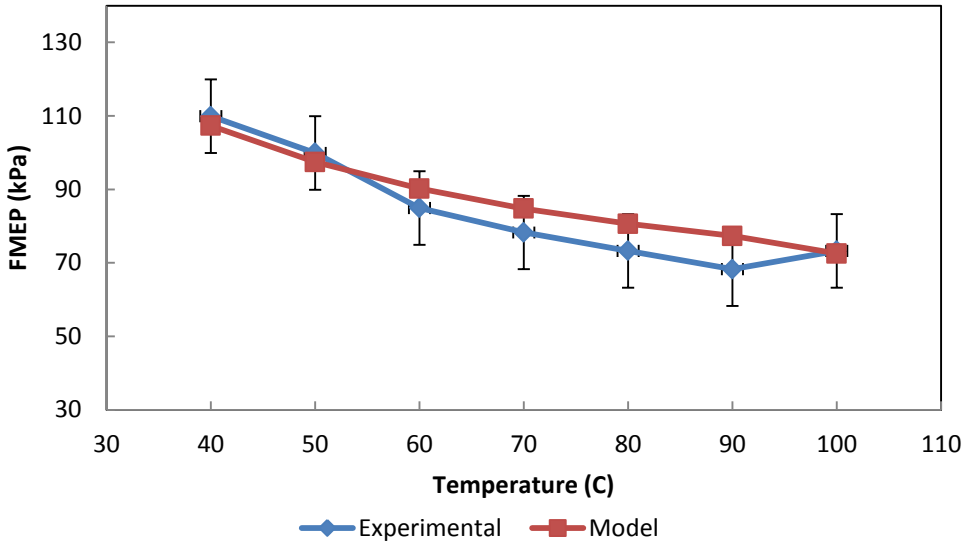

Figure 6.20. Model vs. experimental results for oil SAE 10W40 at 3000rpm

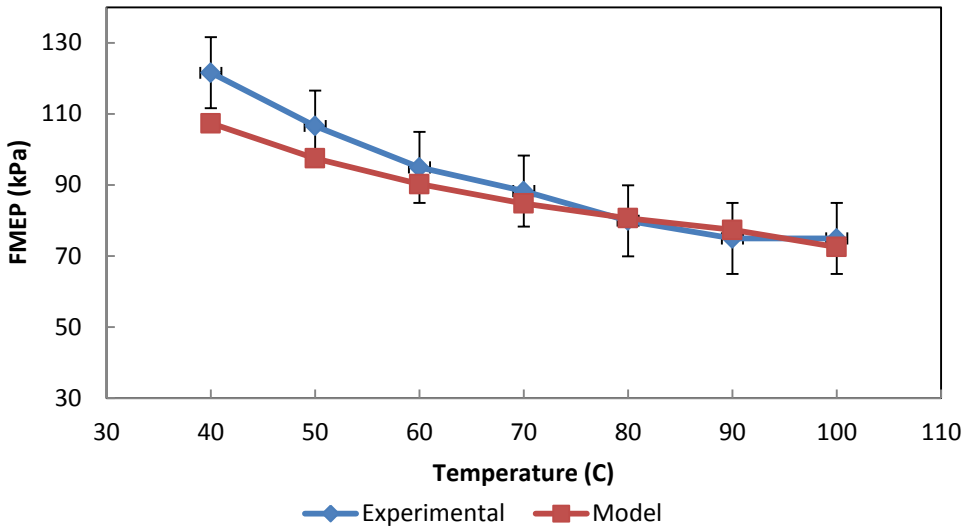

Figure 6.21. Model vs. experimental results for oil SAE 30 at 3000rpm

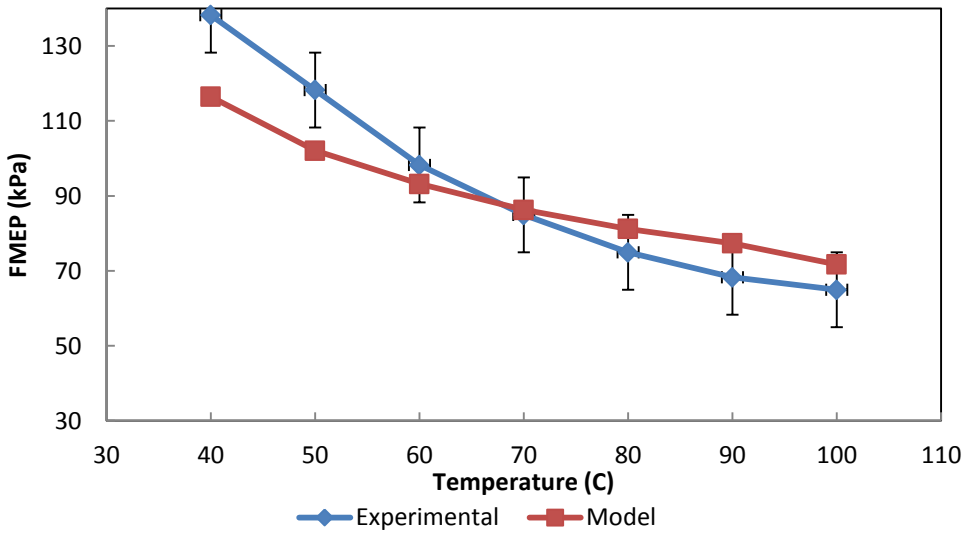

Figure 6.22. Model vs. experimental results for oil SAE 40 at 3000rpm

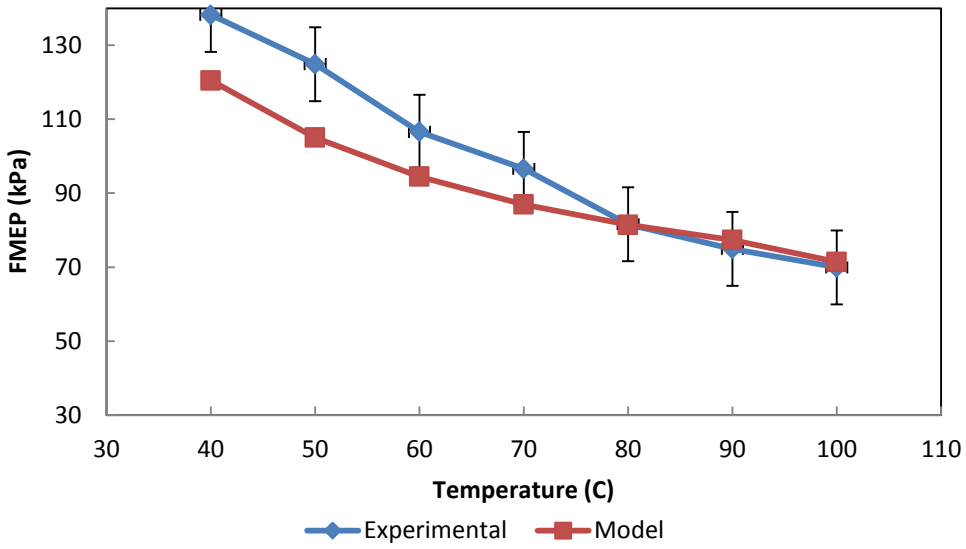

Figure 6.23. Model vs. experimental results for oil SAE 50 at 3000rpm

7. RESULTS FOR ENGINE 2

7.1. BREAKDOWN TEST RESULTS

To test the performance of the modified PNH model against a slight design variation, Engine 2 was subjected to a breakdown motoring test. The results from the breakdown test were compared with the modified PNH model predictions. The Engine 2 has a larger displacement volume, larger bearing sizes and a greater number of valves when compared to the Engine 1. The Engine 2 was tested in four stages, starting with the crankshaft and adding the oil pump, valvetrain and the piston assembly respectively. SAE 10W30 was used as the lubricating oil for this test. The temperature of the lubricant was monitored throughout the complete breakdown motoring test. Figure 7.1 shows the results from the breakdown test on the Engine 2.

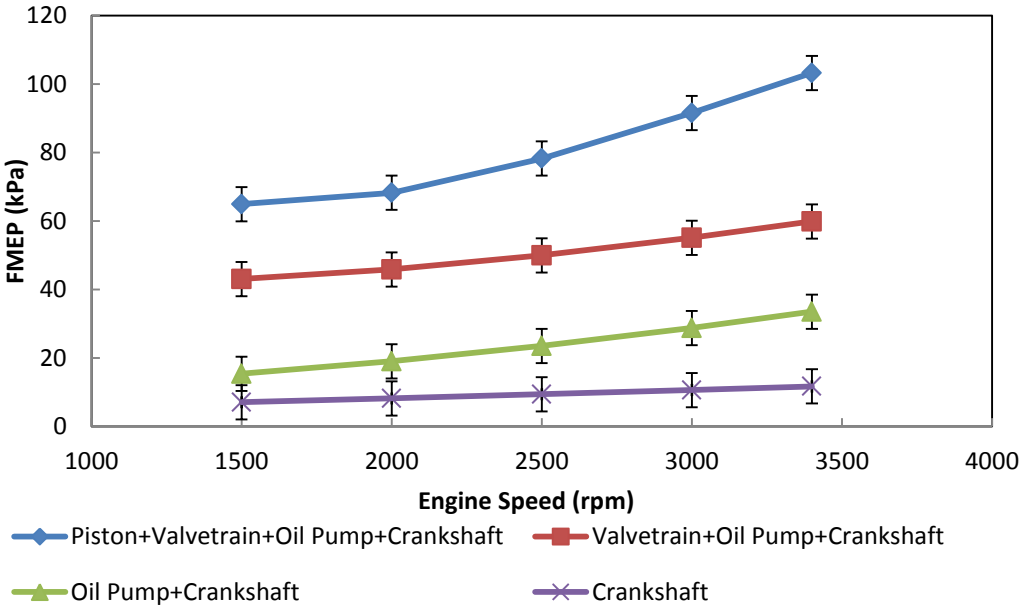

Figure 7.1. Motoring FMEP at different speeds

7.2. PNH MODEL RESULTS

Engine 2 is larger engine in comparison to Engine 1. Therefore, the engine friction is expected to be higher than Engine 1. The complete rubbing friction for Engine 1 ranges between 47.25 to 77.79 kPa between the engine speeds of 1500 to 3400 rpm. Likewise, the corresponding rubbing friction for Engine 2 is between 64.93 to 103.94 kPa. A significant increase in the rubbing friction associated with Engine 2 can observed. Figure 7.2 shows that the modified PNH model successfully predicts the elevated rubbing friction associated with Engine 2. The comparison of experimental versus modified model results of the sub-assemblies has been listed in Section 7.3.

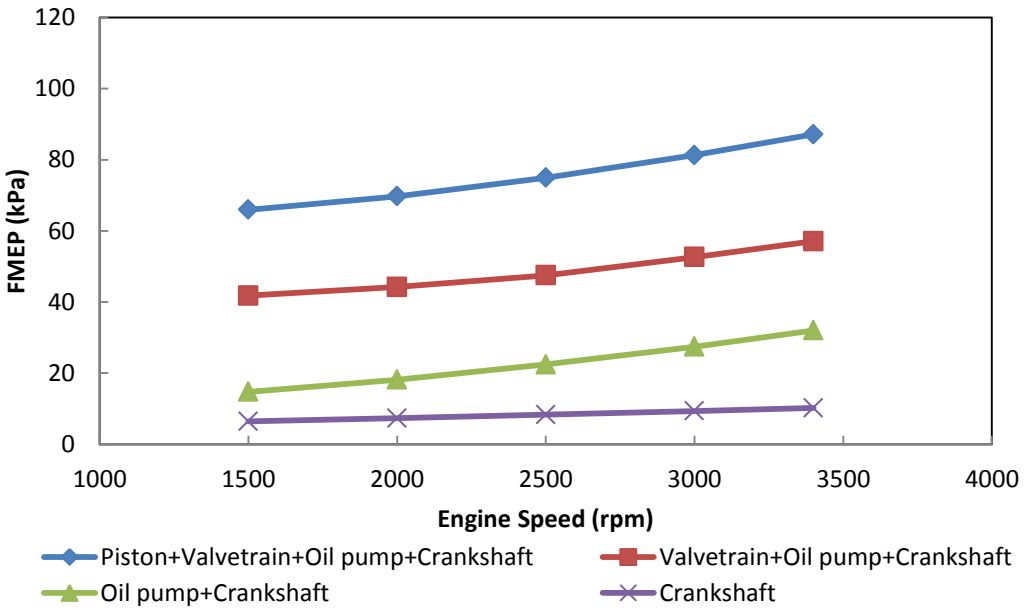

Figure 7.2. Model FMEP at different speeds

7.3. COMPARISION BETWEEN THE BREAKDOWN TEST AND MODIFIED MODEL RESULTS

The comparison between the experimental results and modified PNH model for different components between the temperature ranges 70^{o}C for Engine 2 is shown in the graphs below. The speed range for this breakdown test was between 1500 to 3400 rpm. Figures 7.3 to 7.6 show good agreement between the experimental results and the predictions from the modified PNH model for different sub-assemblies. The use of the physical dimensions for the engine components makes the modified model capable of accommodating the change in bearing dimensions, number of valves and larger displacement volume between Engine 1 and Engine 2. Apart from the design changes the modified model also compensates for the temperature change, as the Engine 2 was tested at 70^{o}C.

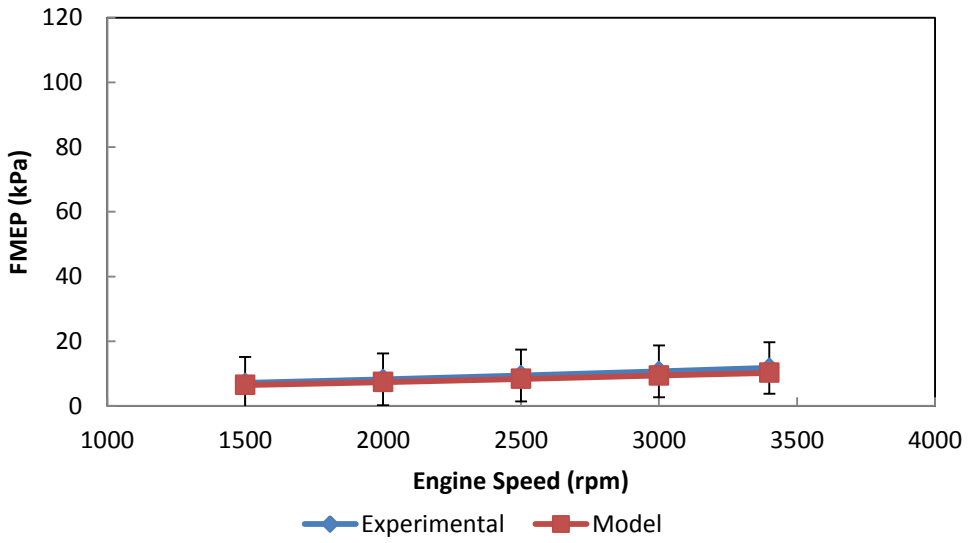

Figure 7.3. Experimental vs. modified model friction for crankshaft assembly

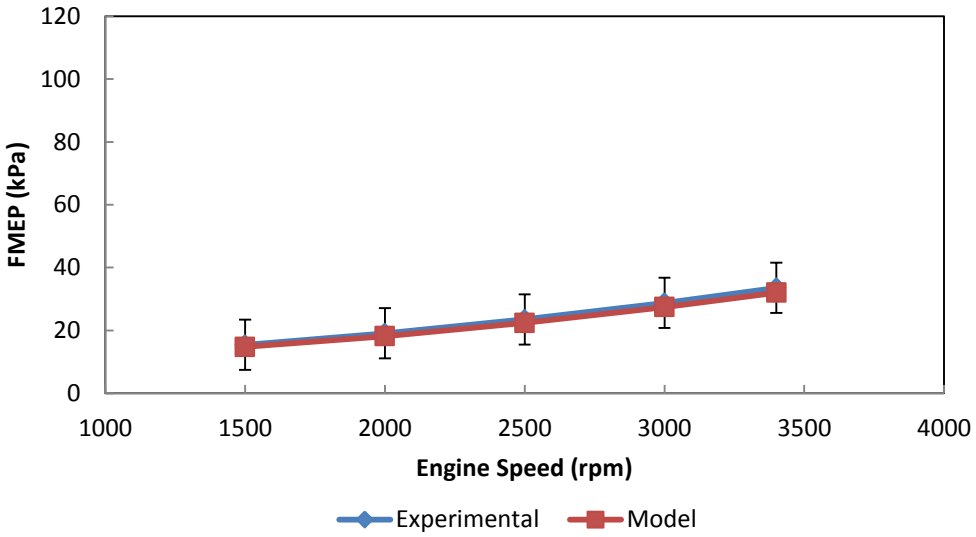

Figure 7.4. Experimental vs. modified model friction for crankshaft, oil pump

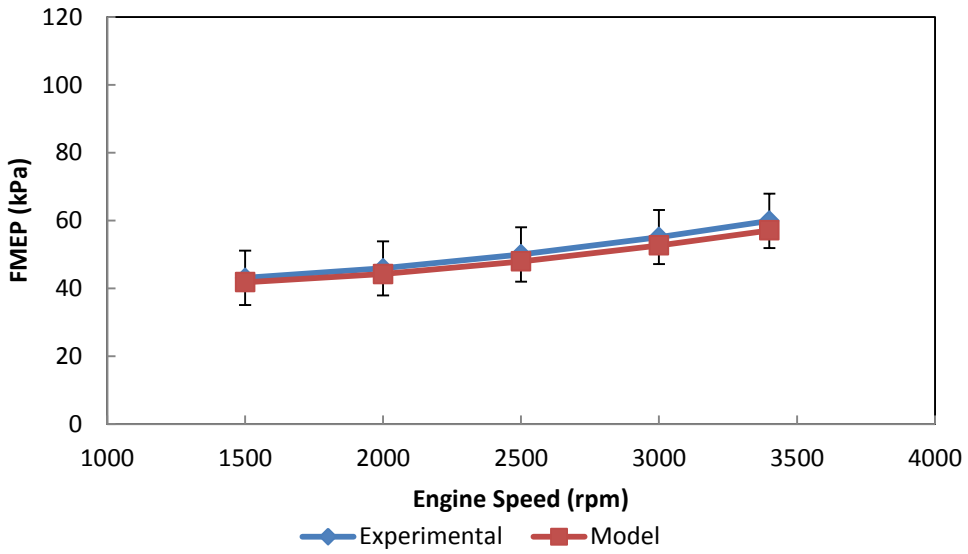

Figure 7.5. Experimental vs. modified model friction for crankshaft, oil pump and valvetrain

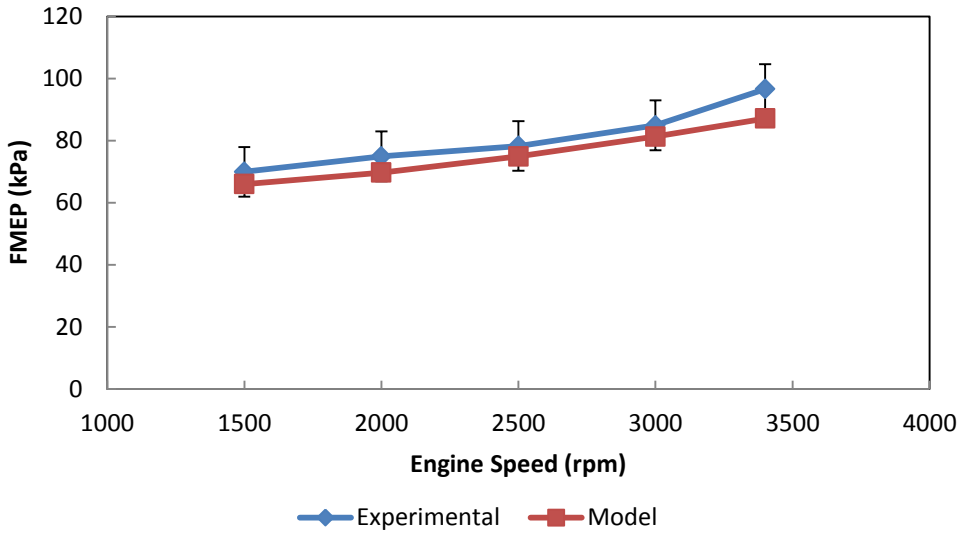

Figure 7.6. Experimental vs. modified model friction for crankshaft, oil pump, valvetrain and piston group

8. SUMMARY

8.1. SUMMARY OF THE MODIFIED PNH MODEL

The results from Engine 1 and Engine 2 prove that the model successfully predicts the rubbing friction associated with the different sub-assemblies of small air cooled SI engines. The model also accounts for the variation in the viscosity of the oil with changing temperature and oil grades. A summary of the experimental results is shown in Figure 8.1. It gives the variation of the total engine rubbing friction with temperature and engine speed for Engine 1.

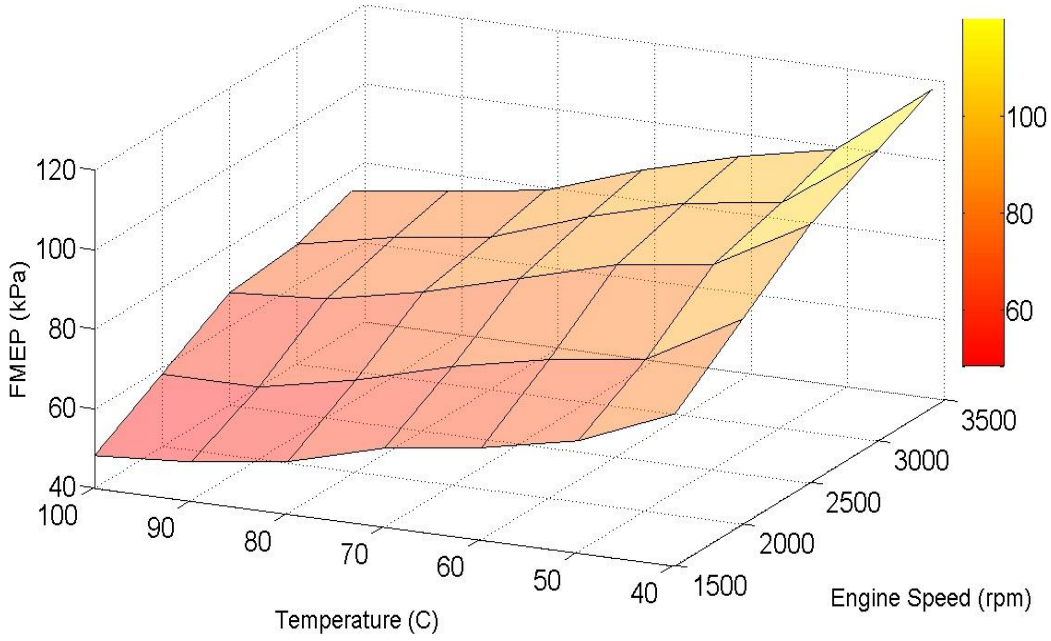

Figure 8.1. Variation of FMEP with temperature and engine speed

A complete modified equation of all the sub-models has been scripted below. All the individual term can be added together to acquire the total rubbing friction FMEP.

$$\mathrm{CMEP}=\left(1.22\times10^{5}\left(\frac{D_b}{B^2Sn_c}\right)\right)_{\mathrm{BST}}+\left(3.03\times10^{4}\sqrt{\frac{\mu}{\mu_0}}\frac{ND_b^3L_bn_b}{B^2Sn_c}\right)_{\mathrm{MBHT}}+\left(1.35\times10^{-10}\left(\frac{D_b^2N^2n_b}{n_c}\right)\right)_{\mathrm{TDT}} \tag{57}$$

$$\mathrm{AMEP}=5.06+\left(0.00000145\times N^2\right) \tag{58}$$

$$\mathrm{VMEP}=\left(244\sqrt{\frac{\mu}{\mu_0}}\frac{Nn_b}{B^2Sn_c}\right)_{\mathrm{MBHT}}+\left(1.81\times10^{-2}\left(1+\frac{1000}{N}\right)\frac{kL_vn_v}{V_d}\right)_{\mathrm{FFT}}+\left(0.5\sqrt{\frac{\mu}{\mu_0}}\frac{L_v^{1.5}N^{0.5}n_v}{BSn_c}\right)_{\mathrm{OHLT}}+\left(\left(1+\frac{1000}{N}\right)\frac{kL_v^2n_v}{V_d}\right)_{\mathrm{OMLT}} \tag{59}$$

$$\mathrm{RMEP}=\left(294\sqrt{\frac{\mu}{\mu_0}}\left(\frac{S_pL_s}{B^2}\right)\right)_{\mathrm{PST}}+\left(\left(1+\frac{1000}{N}\right)\frac{1}{B^2}\right)_{\mathrm{PRFT}}+\left(3.03\times10^{4}\sqrt{\frac{\mu}{\mu_0}}\frac{ND_b^3L_bn_b}{B^2Sn_c}\right)_{\mathrm{HJBT}}+\left(6.89\frac{P_i}{P_a}\left[0.088r_c+0.182r_c^{(1.33-KS_p)}\right]\right)_{\mathrm{GPLT}} \tag{60}$$

9. CONCLUSION

9.1. FRICTION PREDICTION PERFORMANCE OF THE MODIFIED PNH MODEL

The PNH model was tested and modified based on the results from the breakdown test of the Engine 1. Subsequently, the viscosity scaling was applied to the modified PNH model. The model was calibrated at 90^{o}C with SAE 10W30 as the lubricant. Further validation of the model along with the viscosity scaling was accomplished through the temperature variation test on the Engine 1. A breakdown motoring test was also conducted on the Engine 2 to verify the performance of the modified PNH model against a slight design variation. The results prove that the model successfully predicts the rubbing friction associated with the different sub-assemblies of small air cooled engines. The model also accounts for the variation in the viscosity of the oil with changing temperature and oil grades. In addition to a robust rubbing friction prediction model, a breakdown testing procedure was also established to aid the determination of the rubbing friction associated with the individual components of the engine.

9.2. MODEL LIMITATIONS

The rubbing friction prediction model performs well close to the actual operating temperatures. The limitation of this model is to faintly under predict the rubbing friction at lower temperatures. At lower temperatures the oil flow is constrained due to the high viscosity of the lubricant, which causes the rubbing friction to rise more than the prediction from the model. Also, the valvetrain sub-model was calibrated and modified only for an OHV (Over-Head Valve) configuration. The performance of the model might vary with different valve configuration.

APPENDIX A

INPUTS TO THE MODIFIED PNH MODEL

Table A.1: Inputs parameters

Bore	**The Bore diameter of the largest cylinder in mm.**
Stroke	**The Stroke in mm.**
Number of Cylinders	**This is the total number of cylinder present in the engine.**
Speed	**The number of revolutions of the crankshaft in a minute. The unit should be in RPM.**
Compression Ratio	**It is the ratio of the maximum and minimum cylinder volume.**
Intake Pressure	**The intake manifold pressure in kPa.**
Ambient Pressure	**The atmospheric pressure in kPa**
Piston Skirt Length	**The length of the piston skirt in mm.**
Valve Spring Constant	**The highest valve spring constant among the valve springs present in the engine. The units should be kN/m.**
Number of Valves	**Total number of valves in the engine.**
Valve Lift	**The maximum valve lift in mm.**
Oil Viscosity Ratio	**It is the square root of the ratio of viscosities of oil, at two different temperatures. A list of the oil viscosity ratios has been provided in Sheet "Oil Viscosity Ratio".**
Displacement Volume	**The total displacement volume of the engine in cubic meters.**

Apart from the inputs described above, the model also requires bearing information of the crankshaft and the reciprocating (piston) assembly. The bearing inputs for the crankshaft include the diameter, length and the number of bearings on the PTO (Power Train Output) side. The Other side ball bearing was neglected due to its insignificant contribution to the rubbing friction.

APPENDIX B

ADDITIONAL PLOTS

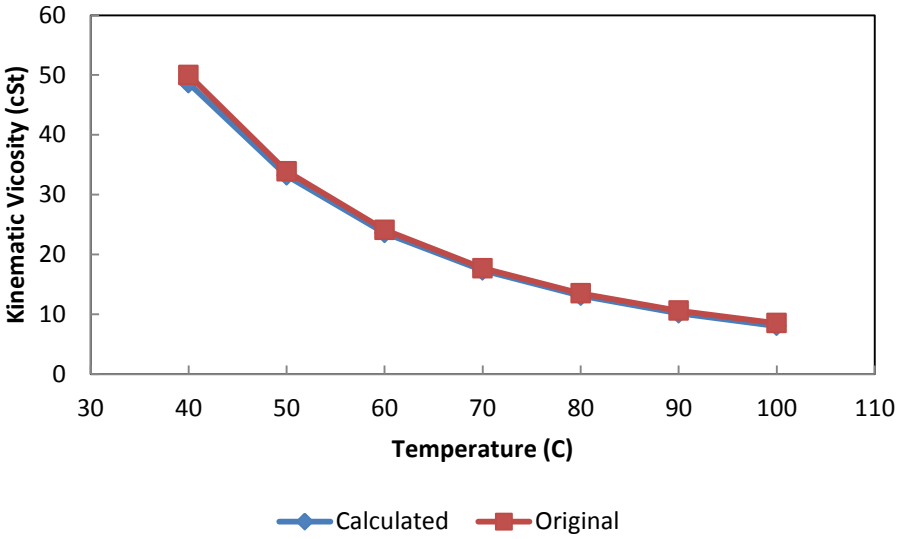

Figure B.1. Viscosity prediction through Vogel's equation for SAE5W20

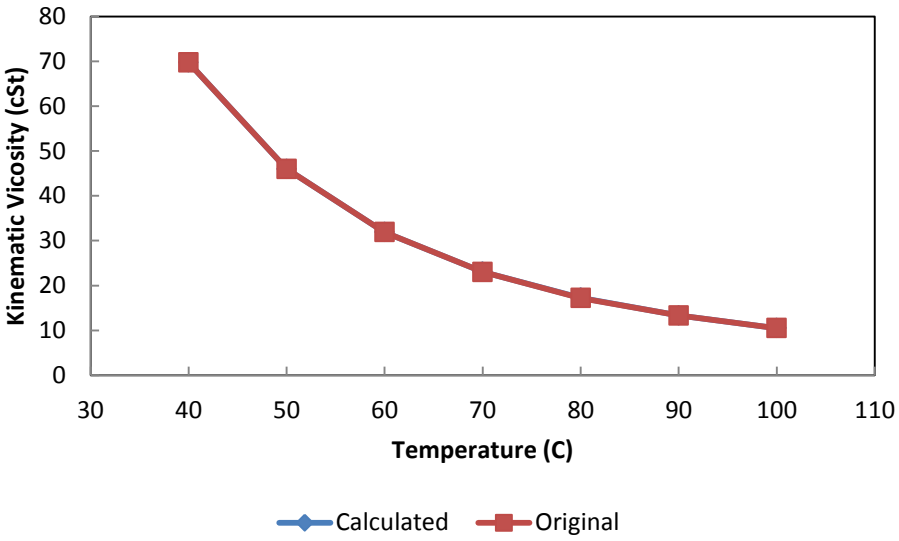

Figure B.2. Viscosity prediction through Vogel's equation for SAE10W30

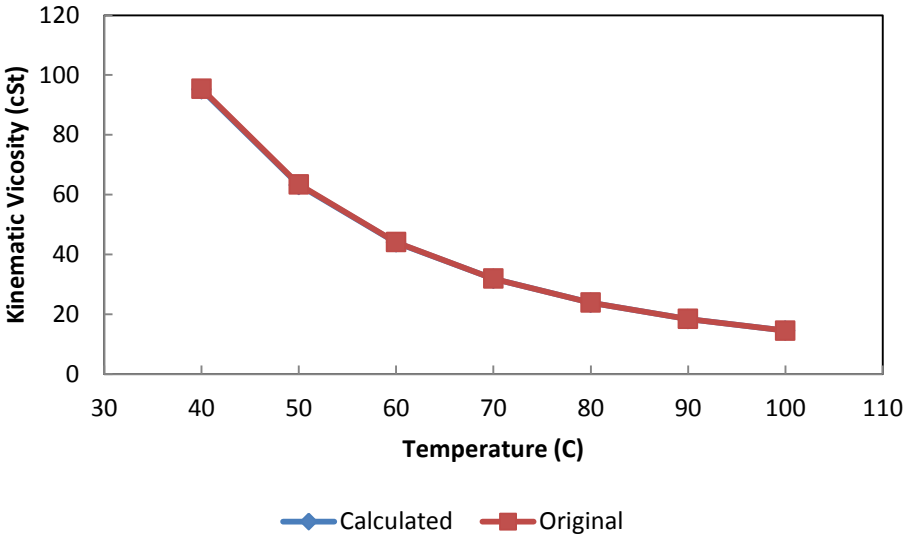

Figure B.3. Viscosity prediction through Vogel's equation for SAE10W40

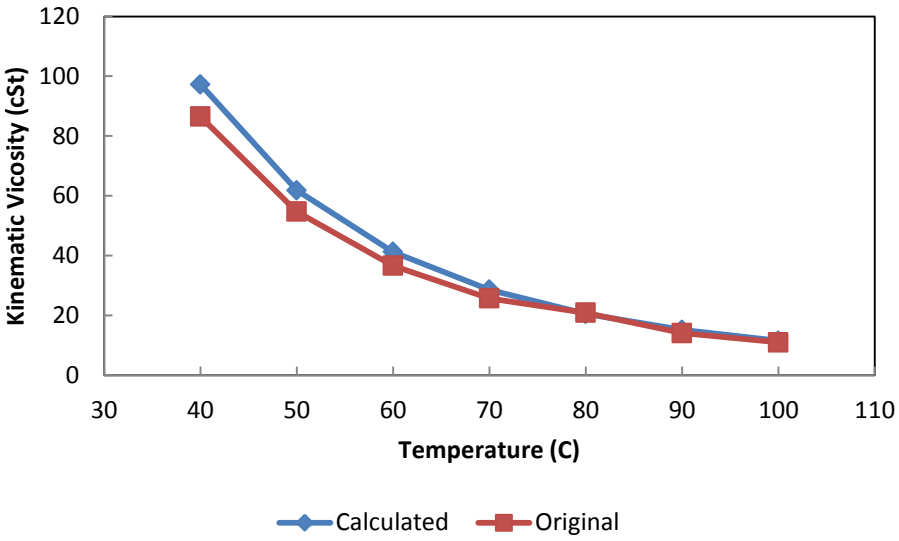

Figure B.4. Viscosity prediction through Vogel's equation for SAE30

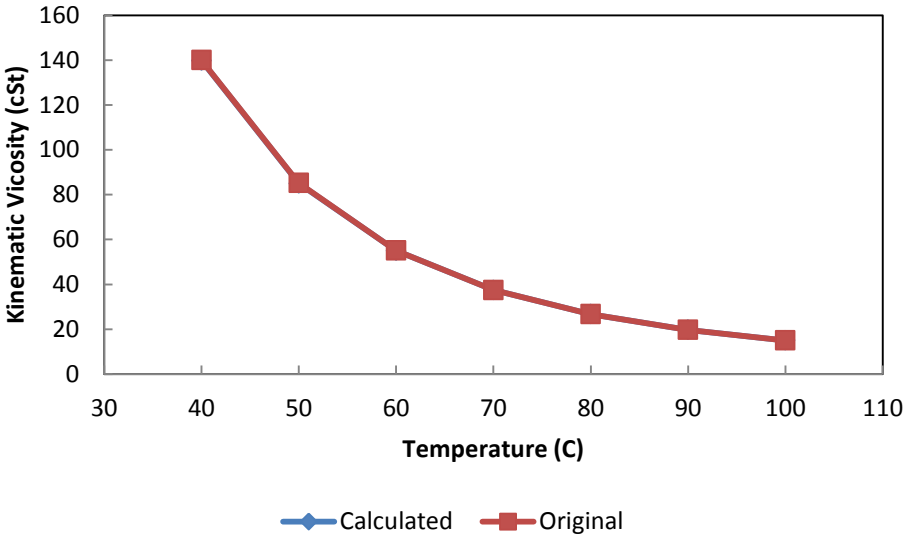

Figure B.5. Viscosity prediction through Vogel's equation for SAE40

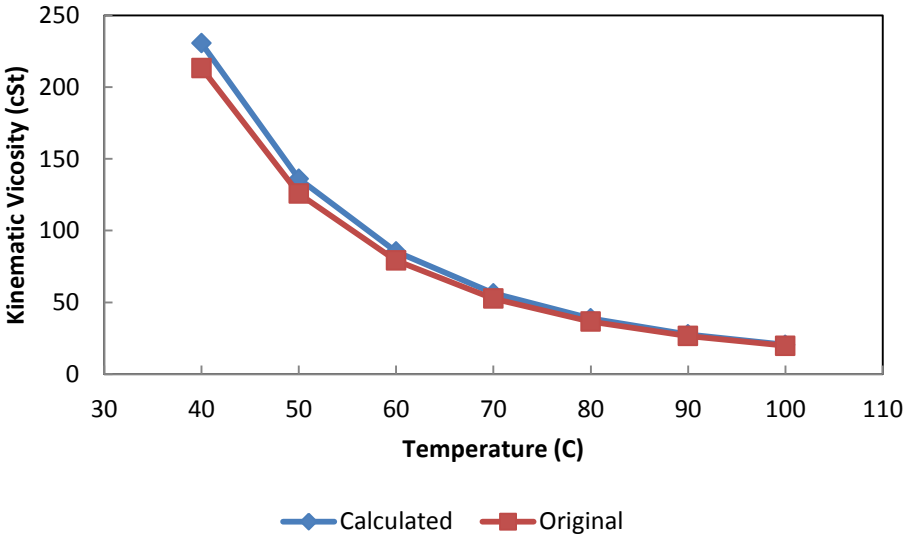

Figure B.6. Viscosity prediction through Vogel's equation for SAE50

BIBLIOGRAPHY

[1] R. E. Gish, J. D. McCullough, J. B. Retzloff and H. T. Mueller, "Determination of true engine friction," SAE Paper Vol. 66. 580063, 1958.

[2] Patton, Nistchke and Heywood, "Development and evaluation of friction model for spark ignition engines," SAE Paper 890836, 1989.

[3] J. B. Heywood, Internal Combustion Engines Fundamentals, McGraw-Hill Book Company, 1988.

[4] Sandoval and Heywood, "An improved friction model for spark-ignition engines," SAE Paper 2003-01-0725, 2003.

[5] Takiguchi and Tomizawa, "Effect of piston and piston ring designs on the piston friction forces in diesel engines," SAE Paper 810977, 1981.

[6] M. T. Shoichi Furuhama, "Measurement of Piston Frictional force in actual operating Diesel Engine," SAE Paper 790855, 1979.

[7] R. V. Basshuysen, Internal Combustion Engine Handbook, SAE International, 2004.

[8] A. Cameron, The Principles of Lubrication, Wiley, 1966.

[9] I.N.Bishop, "Effect of design variables on friction and economy," SAE Paper 812A, 1964.

[10] J. A. William, Engineering Tribology, New York: University Press, 1994.

[11] Uras and Patterson, "Measurement of piston and ring assembly friction instantaneous IMEP method," SAE Paper 830416, 1983.

[12] R. C. Rosenberg, "General friction consideration for Engine design," SAE Paper 821576, 1982.

[13] Wakuri, Ejima, Hamatake and Kitahara, "Studies of friction characteristics of reciprocating engines," SAE Paper 952471, 1995.

[14] Knopf, Eiglmeier and Merker, "Calcutaion of unsteady hydrodynamic lubrication and surface contact at the piston-ring/cylinder liner interface," SAE Paper 981402, 1998.

[15] Stanley, Taraza, Henein and Bryzik, "A simplified friction model of the Piston ring assembly," SAE Paper 1999-01-0974, 1999.

[16] Y. A. O. K. Shimada, "Development of friction prediction procedure for SI engines," F2006P305, 2006.

[17] Kovach, Tsakiris and Wong, "Engine friction reduction for improved fuel economy," SAE Paper 820085, 1982.

[18] R. H. Thiring, "Engine friction modeling," SAE Paper 920482, 1992.

[19] Soejima, Wakuri, Kitahara, Ejima and Nakata, "Studies on the measuring method of the total friction loss of internal combustion engine," JSAE review, vol. 15, no. 1994, 1994.

[20] Shimada, Abou, Okita and Chuubachi, "Development of Friction Prediction Procedure and Friction Reduction Technologies for New Nissan HR and MR Engines," SAE Paper 2006-01-0618, 2006.

[21] Leong and Murphy, "Investigations of Piston Ring Pack and Skirt Contribution to Motored Engine Friction," SAE Paper 2008-01-1046, 2008.

[22] E. J.T.Kovach and L.T.Wang, "Engine friction reduction for improved fuel economy," SAE Paper 820085, 1982.

[23] Singh, Avinash, Huck, Cory H. Wildhaber, Shawn N. Drallmeier, James A., 2011, "Small Engine Design for Fuel Efficiency-Progress Report 7," Missouri University of Science and Technology.

[24] Wildhaber, Shawn N., 2011, "Impact of Combustion Phasing on Energy and Availability Distributions of an Internal Combustion Engine," M.S. thesis, Department of Mechanical Engineering, Missouri University of Science and Technology.

VITA

Avinash Singh was born at Pali, Rajasthan in India to Hemprabha and Anil Kumar Singh. He completed his undergraduate degree in Mechanical Engineering from Bangalore Institute of Technology located in Bangalore. Subsequently, he moved to Missouri University of Science and Technology, Rolla in fall 2009 to pursue Master's in Mechanical Engineering.